DECEMBER 2022

IN COMPLIANCE™

THE COMPLIANCE INFORMATION RESOURCE FOR ELECTRICAL ENGINEERS

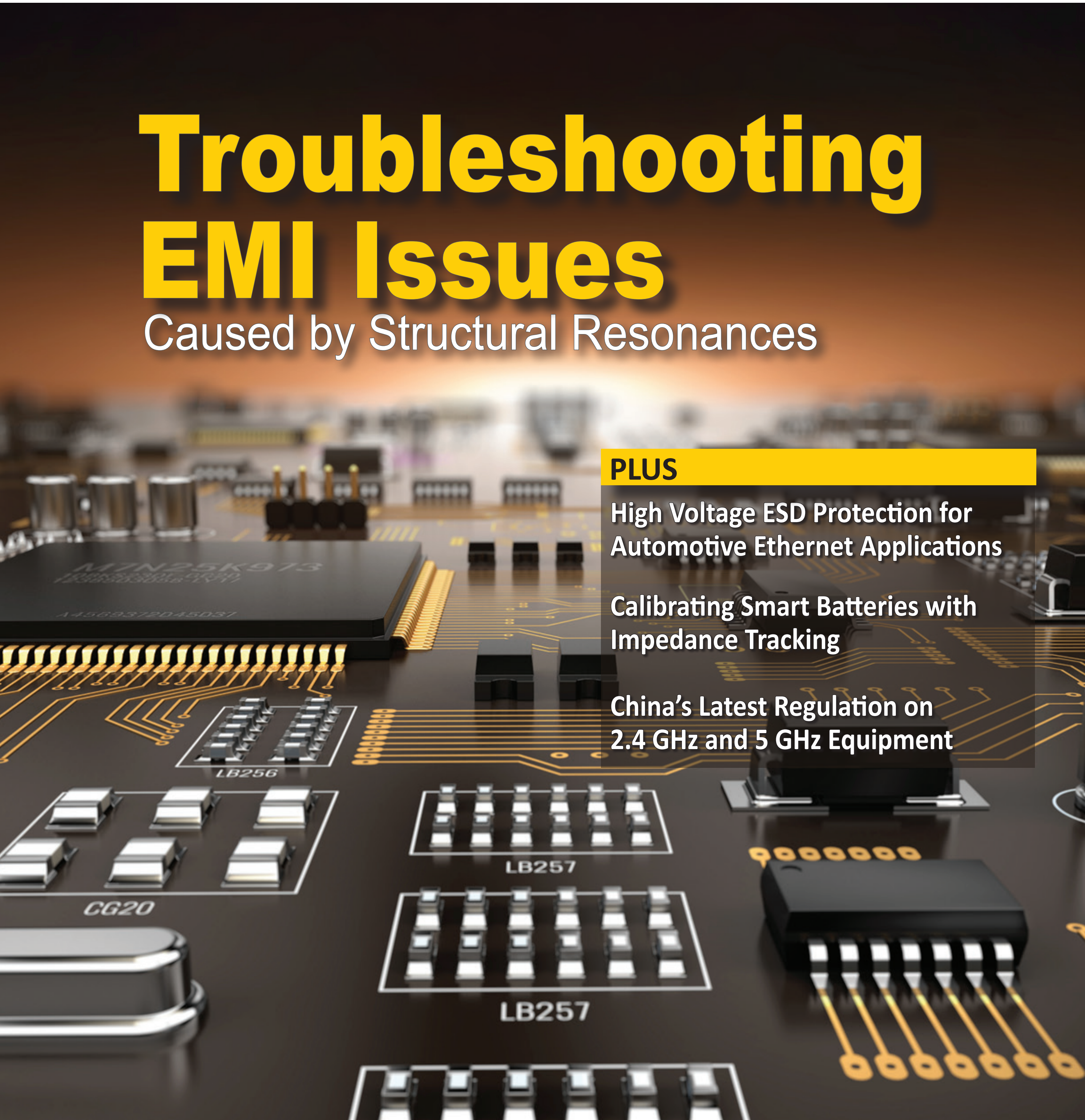

Troubleshooting EMI Issues

Caused by Structural Resonances

PLUS

High Voltage ESD Protection for Automotive Ethernet Applications

Calibrating Smart Batteries with Impedance Tracking

China's Latest Regulation on 2.4 GHz and 5 GHz Equipment

In Compliance Magazine
ISSN 1948-8254 (print)
ISSN 1948-8262 (online)
is published by

Same Page Publishing Inc.
451 King Street, #458
Littleton, MA 01460
tel: (978) 486-4684
fax: (978) 486-4691

IN COMPLIANCE

advertising
For information about advertising contact Sharon Smith at sharon.smith@incompliancemag.com.

subscriptions
In Compliance Magazine subscriptions are free to qualified subscribers in North America. Subscriptions outside North America are $129 for 12 issues. The digital edition is free. Please contact our circulation department at circulation@incompliancemag.com

PRINTED WITH SOY INK

DECEMBER 2022 CONTENTS

Volume 14 | Number 12

EU Will Require USB-C Phone Chargers by 2024

The European Parliament has overwhelmingly adopted a proposal by the Commission of the European Union (EU) that will mandate the use of USB-C charging ports in smartphones, tablets, and other consumer electronics by 2024.

In a vote earlier this month, the Parliament adopted the Commission's recommendation to amend EU Directive 2014/53/EU (also known as the Radio Equipment Directive, or RED) to harmonize charging technologies by standardizing the use of USB-C charging ports. The Commission's proposal would also harmonize supported speeds of charging devices and unbundle the sale of chargers from the sale of electronic devices.

The tally of the Parliament vote was 602 votes in favor of the Commission's proposal, 13 against, and 8 abstentions. The proposal now makes its way to the EU Council for final approval, with publication in the Official Journal of the European Union to follow.

The Commission's proposal is reportedly part of its overall effort to reduce consumer inconvenience and electronic waste created by the use of different and incompatible charging technologies for electronic devices. The Commission estimates that the average consumer owns three mobile phone chargers to ensure reliable access to compatible charging technologies, and that disposed chargers constitute 11,000 metric tons of e-waste every year.

FCC Settles Case of License Holder's Foreign Ownership

The Enforcement Bureau of the U.S. Federal Communications Commission (FCC) has announced a settlement with a company over charges that it failed to accurately disclose ownership stakes in the company held by foreign parties.

According to a press release issued by the FCC last month, the company, Truphone, failed to disclose individual investments of more than 5% of the company by Russian investors Alexander Abramov, Alexander Frolov, and Roman Abramovich without prior approval by the Commission. Subsequently, according to the press release, FCC licenses held by Truphone were transferred repeatedly to unvetted foreign parties without accurate disclosure and review by the Commission.

Under the terms of an agreement with the Enforcement Bureau, Truphone will pay a civil penalty of $600,000 and enter into a rigorous compliance program to prevent future violations of FCC requirements. Further, the company is required to divest Abramov, Frolov, and Abramovich of their holdings in Truphone, and to complete FCC-mandated ownership structure filings that will allow the agency to conduct a thorough review of the company's ownership structure.

Finally, Truphone agrees to take whatever steps necessary to prevent any individuals or entities listed on the U.S. Treasury's Specially Designated Nationals and Blocked Persons List from holding any ownership or investment interest in the company at any time in the future.

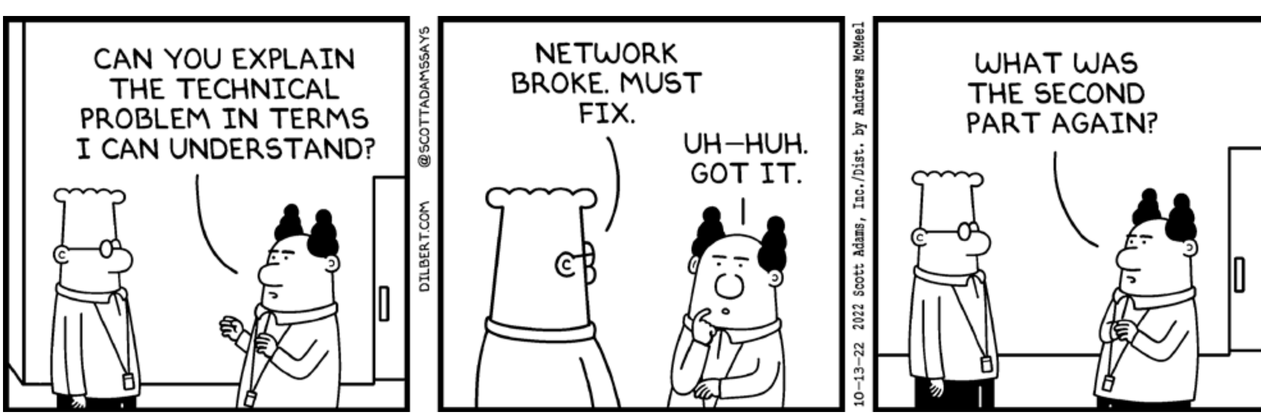

CPSC Publishes Safety Standard for Magnets

The U.S. Consumer Product Safety Commission (CPSC) has approved a new federal safety standard to help reduce human injuries and deaths from swallowed magnets.

Published in the Federal Register, 16 CRF 1262, Safety Standard for Magnets, will now require loose or separable magnets in certain products to be either too large to swallow, or weak enough to reduce the risk of internal injuries when swallowed. The CPSC standard applies to consumer products designed, marketed, or intended for a variety of uses that contain one or more loose or separable magnets. Products exempt from the standard include those distributed solely to school educators, researchers, and/or commercial and industrial users for educational, research, professional, commercial, and/or industrial purposes. The standard also does not apply to toys for children under 14 years of age, since a separate CPSC standard already covers those products.

The mandatory standard came into effect as of October 21, 2022, and will apply to all products manufactured after that date that fall within its scope.

The CPSC says that the products subject to the standard present an unreasonable risk of injury, and that less stringent measures, such as safety messaging, have not been sufficiently effective in helping consumers avoid the potential safety hazards associated with their use. As evidence of the need for a more restrictive standard, the CPSC estimates nearly 27,000 cases of magnet ingestions were treated in hospital emergency rooms from 2010 through 2021, resulting in at least seven deaths.

EU Commission Issues Rules for Automated Driving Systems

The Commission of the European Union (EU) has adopted specific requirements for automated driving systems (ADSs) to help ensure the safety of fully automated vehicles.

Commission Implementing Regulation (EU) 2022/1426 details uniform procedures and technical specifications for the type-approval of ADSs. The specifics of the Implementing Regulation are detailed in four separate annexes, as follows:

- Annex I—Addresses the information that needs to be supplied by the ADS manufacturer in support of their request for EU type-approval;
- Annex II—Sets forth the performance requirements and technical specifications applicable to ADSs under a variety of scenarios and potential operating conditions;
- Annex III—Provides extensive detail on the review process to be used by the relevant approval authorities in their assessment of ADS compliance with the applicable technical specifications, and includes several appendices covering the review of documentation and the tests to be conducted; and
- Annex IV—Maps out the specific requirements for the preparation of an EU type-approval certificate for an ADS that is found compliant with the technical requirements set forth in Annex II.

U.S. DoE to Provide Nearly $3 Billion for EV Battery Development, Manufacturing

The U.S. Department of Energy (DoE) has announced an initial round of funding to expand the domestic development and manufacturing of batteries for electric vehicles (EVs).

According to a press release issued by the DoE, 20 companies based in the U.S. will receive a combined total of $2.8 billion to build and expand commercial facilities in 12 states to extract battery materials, manufacture components, and demonstrate new approaches to battery manufacturing, including manufacturing components from recycled materials.

This initial round of funding represents the first phase of a $7 billion investment in EV batteries authorized under the recently passed federal Infrastructure Investment and Jobs Act, and is intended to support efforts to expand the sale of EVs in the U.S., and achieve a net-zero emissions economy by the year 2050.

Recipient companies of DoE funding will be expected to match the amount of their DoE grant.

FCC Set to Tighten Restrictions Against Huawei, ZTE

The U.S. Federal Communications Commission (FCC) is reportedly on the verge of banning all sales or marketing in the U.S. of telecommunications equipment produced by China telecom companies Huawei and ZTE Corporation.

According to a recent report in The New York Times, the Commission is expected to soon vote on rules that would forbid all sales of new electronics products manufactured by organizations on the FCC's "covered companies" that pose a threat to U.S. national security. The ban would codify a law signed last November by President Biden that prevents the FCC from reviewing or approving any application for equipment authorization produced or manufactured by entities on its "covered companies" list.

Huawei and ZTE were among the first companies named to the FCC's covered companies list in June 2019, a list which now includes 10 separate entities with ties to China. Until now, the extent of the ban on equipment from covered companies has been focused exclusively on prohibiting the use of federal funds to purchase such equipment. The scope of the FCC's reported plan would, in effect, ban all sales of new equipment from covered companies. However, it does not appear that equipment that has already been granted FCC approval would be restricted.

FDA Underfunding May Be Impacting Medical Device Cybersecurity Protections

Insufficient funding and a lack of trained personnel at the U.S. Food and Drug Administration (FDA) may be adversely impacting the agency's ability to thoroughly assess the security of medical devices against cyberattacks.

That's the takeaway from an article posted to the website of MedTechDive. While acknowledging that a draft FDA guidance released earlier this year details the cybersecurity information that manufacturers should supply with their devices in support of the agency's pre-market review process, it notes that many manufacturers view the guidance as optional.

Further, according to some industry experts quoted in the article, devices are being approved by the FDA despite the failure of manufacturers to submit any relevant information about cybersecurity risks and measures they have taken to minimize those risks.

According to the article, the FDA has requested an additional $5.5 million in funding for fiscal year 2023 to develop a more robust program to assess cybersecurity risks in medical devices. Part of the funding would be directed to hiring additional staff that focuses specifically on medical device cybersecurity. But some experts quoted in the article believe that, even with the additional funding, the FDA will still be insufficiently staffed to ensure the thorough review of medical devices for issues related to cybersecurity.

FCC Targets Unauthorized Radio Frequency Devices Once Again

The U.S. Federal Communications Commission (FCC) has cited an online health and wellness company for marketing unapproved radio frequency devices.

According to a Citation and Order issued by the FCC, the Utah-based company Health and Med marketed on its website HealthandMed.com 14 different models of an ionizing footbath featuring digital displays, digital power supplies, and other components that were unintentional radiators. However, the company failed to obtain proper authorization in line with FCC requirements for each of the device models prior to marketing them on their website beginning in 2018.

In its response to an FCC Letter of Inquiry issued in early 2020, the company acknowledged that it sold several of the identified footbath models on its website but did not believe that the devices were subject to FCC regulations. It also noted that it subsequently tested several models of the footbaths in accordance with Part 15 requirements and that the devices passed. However, the FCC notes that the company continues to sell two models of footbaths but has so far failed to provide information to the FCC regarding the authorization for these models.

Under the terms of the Citation, the company has 30 days to provide the FCC with copies of either their authorizations or test results for the devices that are still being marketed.

TROUBLESHOOTING EMI ISSUES CAUSED BY STRUCTURAL RESONANCES

Recognizing the Signs of Structural Resonances

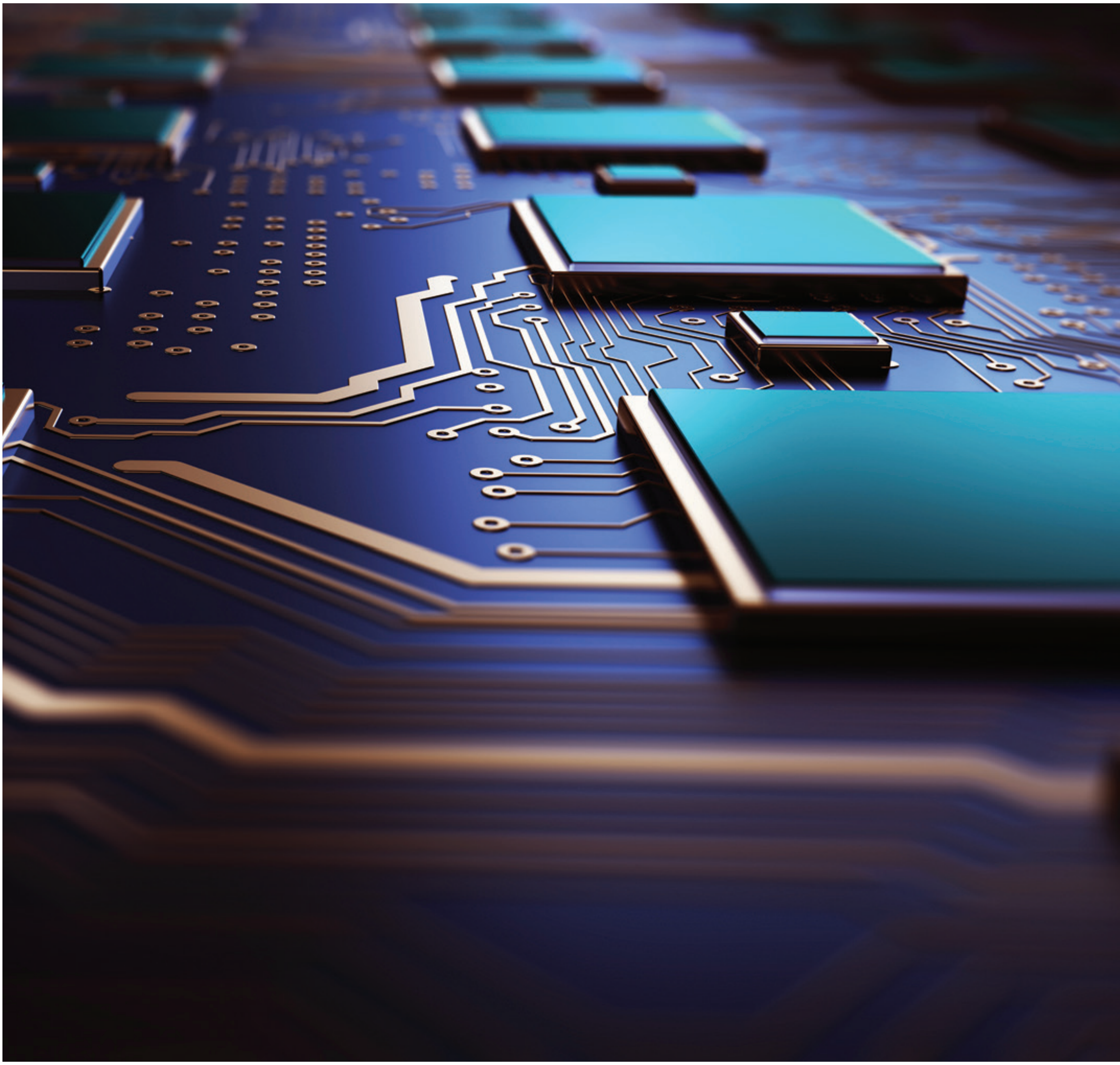

Dr. Min Zhang is the founder and principal EMC consultant of Mach One Design Ltd, a UK-based engineering firm that specializes in EMC consulting, troubleshooting, and training. His in-depth knowledge of power electronics, digital electronics, electric machines, and product design has benefitted companies worldwide. Zhang can be reached at info@mach1desgin.co.uk.

By Dr. Min Zhang

Has it happened to you? When troubleshooting an electromagnetic interference (EMI) issue, you've tried various combinations of components and saw the signal of interest reduced. But another frequency signal unexpectedly raised above the limit line. Or, you introduced a chassis plane on your printed circuit board (PCB), only to find the radiated emissions became much worse instead of getting better. These are typical cases of "tuning the resonances of a circuit."

Most EMI emissions are related to structural resonances. Structural resonances are also one of the main reasons that electromagnetic compatibility (EMC) can be mystifying. Unknowingly, engineers often spend days and months tuning the resonances of a circuit by adding passive elements such as inductors and capacitors. Sometimes, they are lucky enough to finally arrive at a combination that would give them a pass. But most of the time, solutions are hard to find.

A tremendous amount of work has been done on the subject of structural resonances and an overview of these works can be found in Reference 1. Two practical case studies are also presented in Reference 1 to demonstrate methods to identify, locate, and fix EMI issues that are associated with structural resonances.

EMC engineering often requires problems to be resolved (but not studied) within a limited time. Therefore, techniques that are effective but also save time are encouraged. There are indicators that signal the presence of structural resonances, and engineers can learn to use these indicators to locate the resonant structure and fix the EMI issues. This article also explores some practical techniques in troubleshooting EMI issues that are caused by structural resonances. Case studies are presented to illustrate these techniques.

ROOT CAUSES

The following conditions need to be met in order for a structure to resonate:

1. There needs to be a resonant structure. In electrical terms, this means an undamped/lightly damped L-C circuit. Physically, this could mean anything in an electrical system. Two typical cases are shown in Figure 1. As shown, two PCBs that have a cable connection represent an L-C circuit where the inductive component L depends on the length of the cable and the capacitance component C depends on the structure of the PCBs (areas and the distance between the PCBs). For larger system installations such as the one shown in Figure 1(b), L depends on the length of the ground leads of each cabinet and C depends on the area of the side wall of the cabinet and the distance between the two cabinets.
2. There needs to be an excitation source. Translated into EMC terms related to emissions, the excitation source could be any switching source on a PCB or in a system. For immunity, the excitation

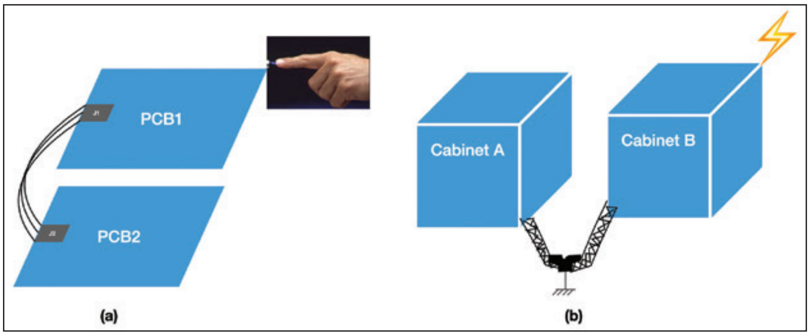

Figure 1: Typical cases of structural resonances; (a) Two PCBs with a wire connection; (b) Two cabinets with the same ground point.

source could be an external RF field, an ESD event, or a lightning strike, as shown in Figure 1.

3. An antenna-like structure can also be treated as a structural resonance depending on the physical size of the conductor. Since an antenna is excited most effectively when the size of the antenna (often a wire) is either one-half or one-quarter the wavelength of the exciting frequency, the physical length of the antenna determines the resonance frequencies.

LOCATING THE STRUCTURAL RESONANCES

Generally speaking, there are three methods to locate structural resonances which include the analytical, frequency domain and time domain techniques.

An analytical approach generally requires experience and technical know-how to model/simulate the system. For small systems with known issues, such as the case study presented in Reference 1, simple mathematical calculations are often good enough to give an estimation of the resonant frequency of the device under test (DUT). Often, an analytical approach is achieved either by 3D full-wave simulation or some specialized EMC software.

The benefit of the analytical approach is that it can make a prediction before a prototype is built, making this approach popular in the design and development of automotive, aerospace, and space applications. Often, such companies have simulation models that have been validated in the past and that can be easily modified for a new study. But for companies that don't have existing models, building a simulation can be a costly and lengthy journey.

In the frequency domain, there are two main techniques. Measuring the reflected power by a magnetic field loop is discussed in Reference 2 and the same method was demonstrated in Reference 1. This method requires a small magnetic field loop to "sniff" suspicious structures, often on the PC board level. Williams introduced a far-field measurement using a spectrum analyzer with a tracking generator (see Reference 3). A reference signal is injected into the DUT by the tracking generator output and an antenna is used for measuring the response signal. This method is particularly useful in applications where the PCB ground resonates with the enclosure (chassis). Both methods are practical and only require a small amount of test set-up. The drawback of these methods are they are often limited to PCB board-level investigation and are not useful in large systems.

In the time domain, measuring the resonant current with an RF current monitoring probe when a pulse is injected into the system is often used (see Reference 4). This serves as an effective technique when it comes to troubleshooting large systems or where multiple PCBs are interconnected.

Table 1 summarizes the techniques and pros and cons of each method.

Method	Equipment	Pros	Cons
Analytical assessment	Simulation software such as full wave simulator or specialized EM simulation software	This method allows engineers to "see" the resonance even before the prototype is built.	The learning curve of this software is often long. It takes a long time to accurately build a model. Licence to run the software can be costly.
Measuring reflected power with a small magnetic field loop	Magnetic field loops, a network analyzer or a spectrum analyzer with a tracking generator, a directional coupler	A low-cost measurement and it can be very efficient. As demonstrated in References 1 and 3.	This method has its limitations when it comes to large systems as the magnetic field loops reach their physical limit.
Using a far-field antenna	An antenna, a spectrum analyzer with a tracking generator	Test set-up is relatively easy, the result is straight-forward.	One needs to know where in the system to inject the reference signal.
Measuring resonance using an RF current monitoring probe	RF current probes, an oscilloscope, a pulse generator (such as an ESD simulator or EFT generator)	This is a time domain measurement, suitable for large system installations	High-energy pulse generator is often expensive to buy/rent.

Table 1: Methods of locating structural resonances

One of the typical characteristics of structural resonances is that resonances can increase the amount of emissions because the final radiator is more efficient than the original radiator.

These techniques are introduced and demonstrated in Reference 1. This article further explores more practical approaches based on the characteristics of structural resonances.

RESONANCES INCREASE THE AMOUNT OF EMISSIONS

One of the typical characteristics of structural resonances is that resonances can increase the amount of emissions because the final radiator is more efficient than the original radiator (see Reference 5). The following case study demonstrates the point.

During the radiated emission tests of a large-size electric vehicle, it was found that a narrowband spike at 222MHz exceeded the limit (Figure 2a). It was found that the noise came from a camera that was fitted in the cabin of the vehicle. Multiple ferrites were used on the power leads of the camera, but the improvement was not significant enough to suppress the noise (this is another sign of structural resonances). The test also showed an “inconsistency,” as the same noise was measured a lot lower on some occasions (as shown in Figure 2b). We accidentally discovered that the difference in the emission results was caused by the door of the vehicle. When the door was open, the noise emission was significantly less than when the door was closed.

By themselves, the vehicle cameras and their associated circuitry including the 20 cm long power leads were not an efficient radiator at the frequencies (and the harmonics) contained in the circuits. As shown in Figure 3, when the door was closed, it was positioned near the camera area. The door was mainly glass, but the frame, together with the mechanical structure linking the door, was part of the metal enclosure and should be considered an EMC concern. Even though the door was not in physical contact with the camera, the parasitic capacitance and inductance coupled the RF energy of the camera onto it, and the noise at 222 MHz was radiated very efficiently. At 222 MHz, a halfwave length wire is about half a meter. The structure shown in Figure 3 can easily act as an efficient antenna.

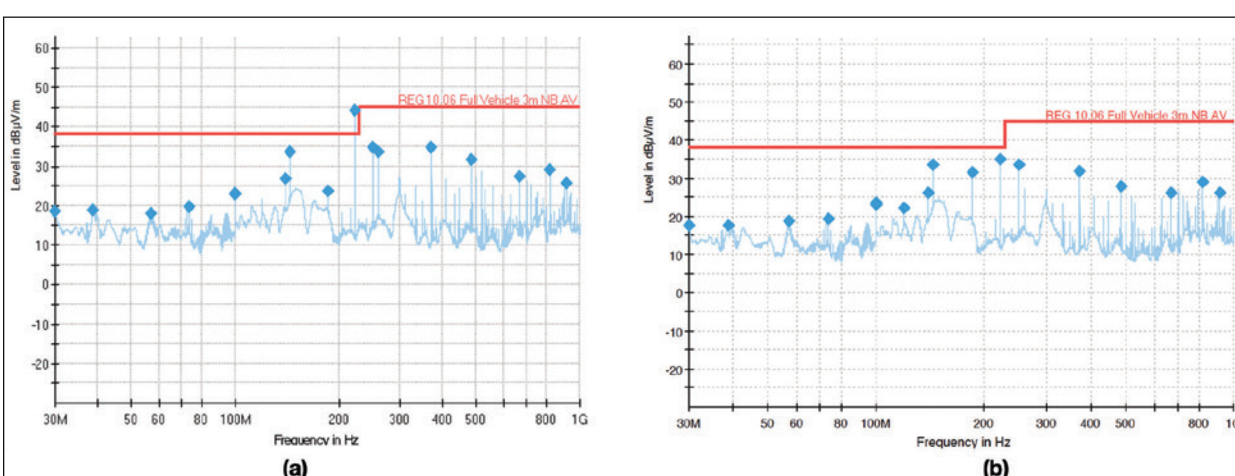

Figure 2: (a) Noise at 222 MHz caused by the in-cabin camera (b) when the door of the vehicle was open

Identifying and locating the structural resonance is often the most difficult part of the job when it comes to EMI troubleshooting.

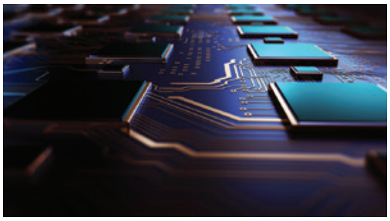

Identifying and locating the structural resonance is often the most difficult part of the job when it comes to EMI troubleshooting. In this case, it makes sense that the ferrites on the camera power leads were not effective as the final radiator was not suppressed. A more sensible approach is to segregate the noise source by shielding the camera power lead with aluminum foil and locating it away from the door. This also serves as a cost-effective way of fixing the issue.

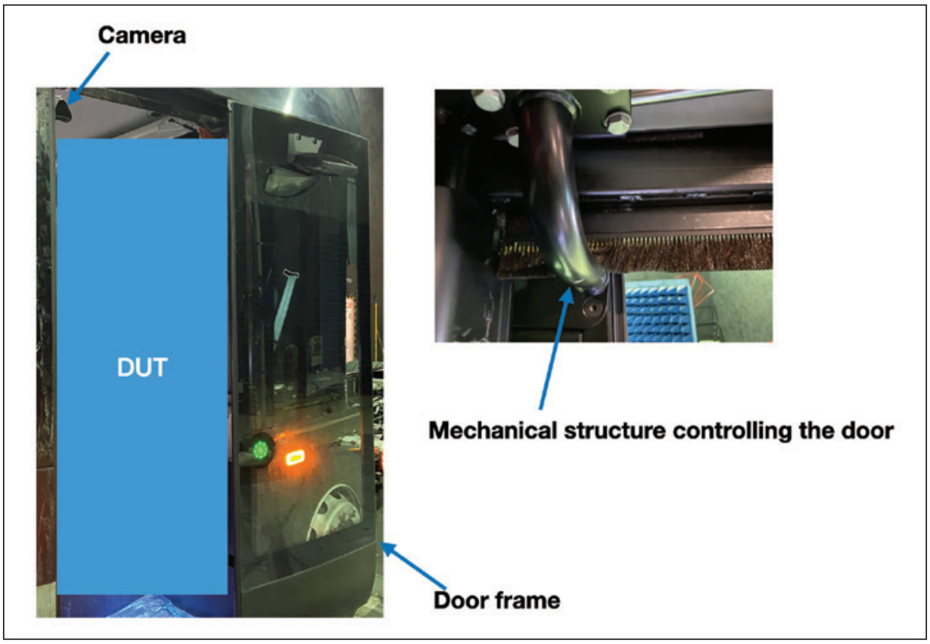

Figure 3: The door of the DUT acts as a more efficient antenna and increases the emissions

The noise was significantly reduced when the door was closed as shown in Figure 4.

RESONANCES ABSORB MORE ENERGY IN IMMUNITY TESTS

In this case study, a device failed the immunity tests (both radiated immunity and bulk current injection (BCI) tests) in the frequency range of 200 and 400 MHz, and the range of 800 and 900 MHz. In other frequency ranges, the device worked as normal without error.

The PCB of the DUT has a size of roughly 50 mm × 50 mm, forming a 200 mm-long loop. The assumption was that traces and tracks on the PCB might have formed an efficient loop antenna within the 200-350 MHz frequency range. Electromagnetic wave travels in an FR4 material at a speed of 1.5×108 m/s, based on equation v=λf, where v is the speed of light in FR4 and f is the frequency. For a 200 MHz wave, a full wavelength is then calculated to be 750 mm. A quarter of wavelength (where the radiation is the strongest) is 187.5 mm. The PCB itself can resonate at a frequency range of 200 MHz. It would probably absorb more RF energy at 200 MHz (and its harmonics) which is injected from the noise source in the immunity tests.

Using an RF current monitoring probe, we measured the RF in front of and behind the PCB in the immunity test, as shown in Figure 5. A frequency sweep was performed from 100 MHz to 1GHz. The RF amplifier injected the same level of RF noise into the main connector cable via a BCI probe from a frequency range of 100 MHz and 1 GHz. The results are shown in Figure 6.

The yellow trace showed results in location 2 and the pink trace showed the results in location 1. The blue trace is the difference between the two measurements. Basically, the positive profile shown in the blue trace (as shown from frequency point markers 1 and 2 and from frequency point markers 3 and 4) means the PCB amplifies the input signal, whereas with the

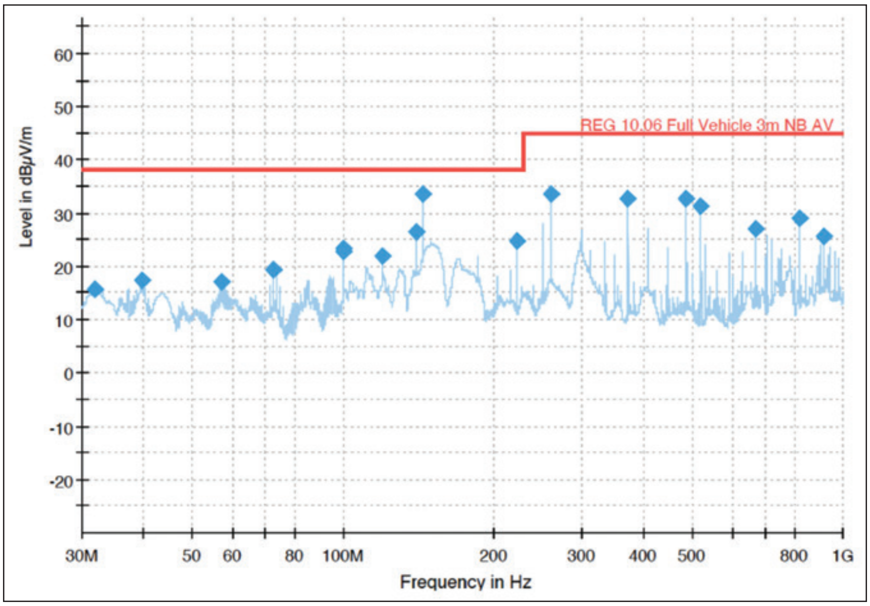

Figure 4: Segregating the camera power leads using aluminum foil, the 222 MHz noise was significantly reduced.

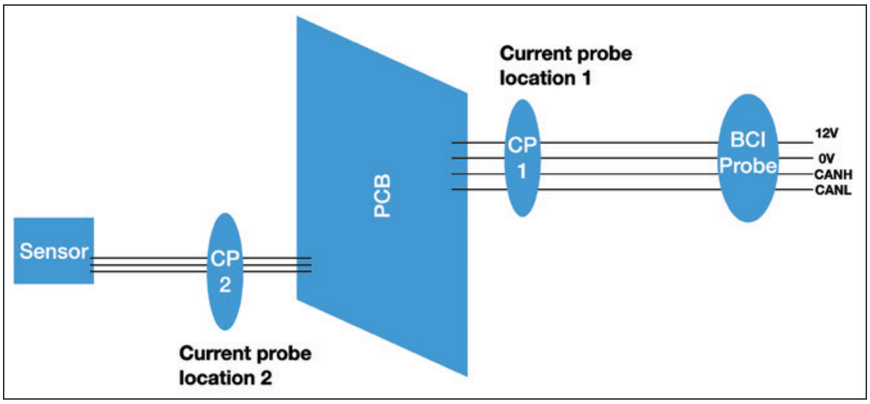

Figure 5: Test set-up to measure the RF current on two locations of the DUT, location 1-before the PCB; location 2 – after the PCB

rest of the frequency range, the PCB attenuates the RF noise (shown as negative profile). We now know why we had an immunity issue between 200 MHz and 400 MHz and between 840-920 MHz.

The solution to this immunity problem requires a common mode choke (CMC) that works most effectively in the frequency range of interest, together with decoupling capacitors. The capacitance values are 470pF as they work effectively in this frequency range.

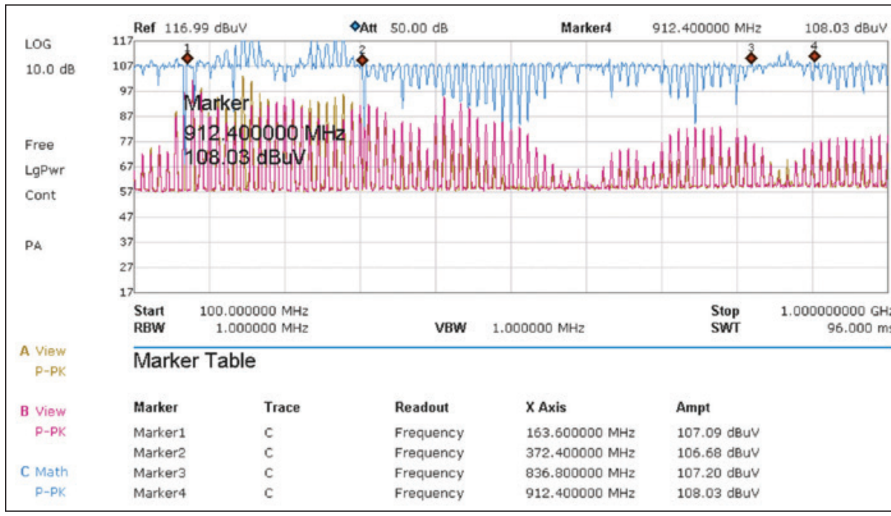

Figure 6: Frequency sweep between 100 MHz and 1 GHz

Using a ferrite as a filter element to reduce cable resonance is usually effective as ferrites are resistive (lossy) and should act as a damping element. But if the main structural resonance is not the cable, adding ferrite sometimes adds reflections.

FERRITES OFTEN DON'T WORK

Another sign of structural resonances is that ferrites often don't work as effectively as they should. For instance, in the first case study, ferrites on the power lead of the camera didn't suppress the noise as one would hope. Using a ferrite as a filter element to reduce cable resonance is usually effective as ferrites are resistive (lossy) and should act as a damping element. But if the main structural resonance is not the cable, adding ferrite sometimes adds reflections. As a result, the noise level stays the same or shifts with frequency.

Figure 7 shows the conducted emission of a newly developed PCB design which created a resonance issue between 50 and 100 MHz.

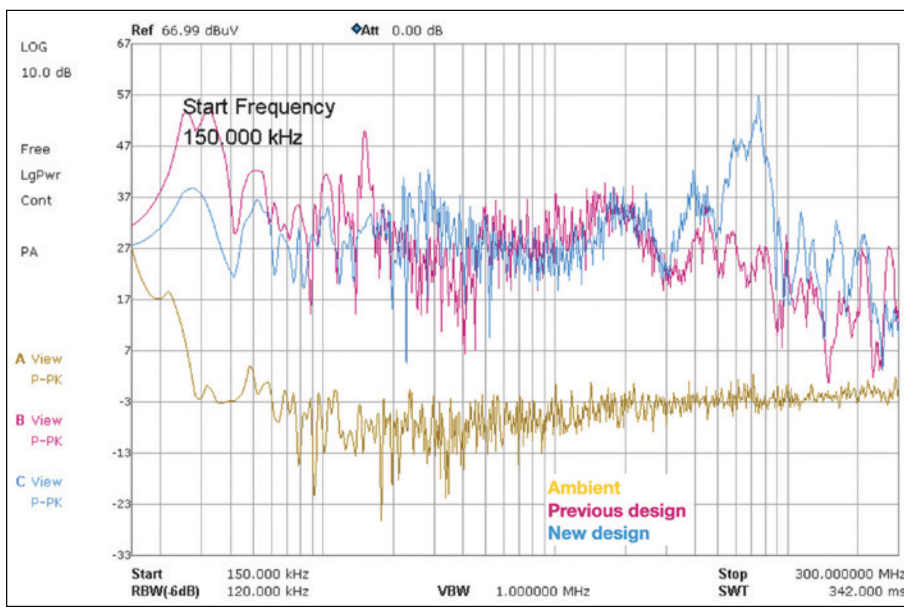

Figure 7: Conducted emission results of the PCB in development; yellow trace – ambient, pink trace – previous design, blue trace – new design

As it can be seen, the new design improved the low-frequency performance of the PCB but failed significantly at high frequency. What the engineers found was that even with multiple ferrites on the

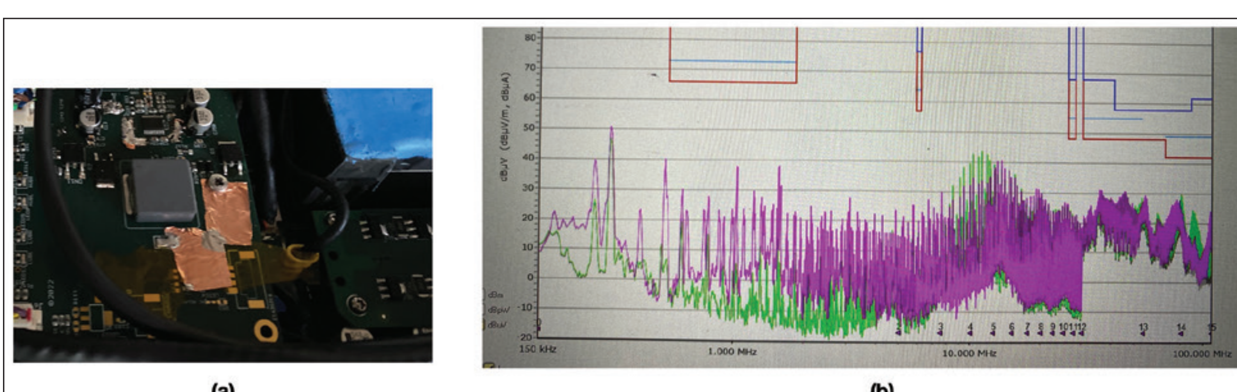

Figure 8: (a) connecting the chassis and the ground plane by copper tape connections (b) the conducted emission results improved significantly

power cable, the conducted emission could not be reduced. In the frequency between 50 and 100 MHz, the noise profile stayed high.

It was found during the layout review that the engineers had neglected to connect the chassis and the ground plane of the PCB. As a result, the ground plane of the PCB started resonating with the chassis when the DUT was in operation. A high dV/dt was developed on the ground plane with reference to the chassis, driving the emissions up. A quick copper tape connection between the ground and chassis points on the PCB (shown in Figure 8a) reduced the noise by more than 20dB in the frequency range of interest (Figure 8b).

CONCLUSION

When troubleshooting EMI issues, there are a few signs that indicate structural resonances. Structural resonances increase emissions in the resonant frequency range (and its harmonics) and they also cause the system under test to be more sensitive to external interference at the resonant frequency. Sometimes, adding ferrites cannot fix the problems caused by structural resonances, and adding capacitors shifts the resonant frequency. The first step in fixing these issues is to identify and locate the resonant structure. Once this is done, solving the problems often involves isolation, damping, and improving the ground connections.

REFERENCES

1. M. Zhang, "Structure Resonances: Ways To Identify, Locate, and Fix EMI Issues," *Signal Integrity Journal*. https://www.signalintegrityjournal.com/articles/2420-structure-resonances-ways-to-identify-locate-and-fix-emi-issues
2. D. Smith, "Measuring Structural Resonances," https://emcesd.com.
3. T. Williams, "Controlling Resonances in PCB-Chassis Structures."
4. D. Smith, "Measuring Structural Resonances in the Time Domain," https://emcesd.com.
5. B.R. Archambeault, *PCB Design for Real-World EMI Control*, Kluwer Academic Publishers, Norwell, Massachusetts, 2002.

HIGH VOLTAGE ESD PROTECTION FOR AUTOMOTIVE ETHERNET APPLICATIONS

IEEE and OPEN Alliance Standards and Testing

Andreas Hardock is the Application Marketing Manager at Nexperia, with a focus on ESD and EMC issues impacting the automotive domain. Hardock studied nanostructure technology at the Julius Maximilian University of Würzburg and earned his Ph.D. in the field of functional vias at the Technical University of Hamburg-Harburg. Hardock can be reached at andreas.hardock@nexperia.com.

By Andreas Hardock

Ethernet solutions have been popular in industrial and computing applications for several decades but were not widely adopted in the automotive area. Automotive Ethernet enables fast and robust data communication, with high flexibility in bus topologies for multiple electronic control units (ECUs). This makes Ethernet technologies a potential candidate to provide high bandwidth, connectivity, and robust operation while accelerating the evolution of automotive networks from domain to zonal architecture.

In 2016, two standards, 100BASE-T1 and 1000BASE-T1, were drafted for the automotive industry. As of 2022 two additional standards, namely 10BASE-T1s and MGB-T1, are in development by the One Pair Ethernet Network (OPEN) Alliance committees. OPEN Alliance includes several technical committees for the standardization of Ethernet-based technologies in the automotive market. The Institute of Electrical and Electronic Engineers (IEEE) covers 100BASE-T1 and 1000BASE-T1 with the IEEE 802.3bw and IEEE 802.3bp standards. Both were adopted to serve specific automotive requirements, mostly related to electromagnetic compatibility (EMC).

This article will look at the requirements and properties of modern semiconductor electrostatic discharge (ESD) protection devices in connection with the requirements detailed in 100BASE-T1 and 1000BASE-T1. We'll highlight how ESD protection devices act in synergy with the rest of the circuitry resulting in a robust system against destructive ESD and EMC.

REQUIREMENTS ON ESD PROTECTION FOR 100BASE-T1 AND 1000BASE-T1

The high flexibility of Ethernet connections is an advantage for automotive applications. It can be used in a star topology, that is, having a switch as a central point connected to several domains, e.g., ADAS, Infotainment, or other. It also works in a bus topology as has been used in traditional CAN and FlexRay applications.

A typical bus configuration can include multiple Ethernet nodes as shown in Figure 1, which shows advanced driver-assistance systems (ADAS) with sensors in the front and displays in the car interior. It is crucial to understand that the standardization of

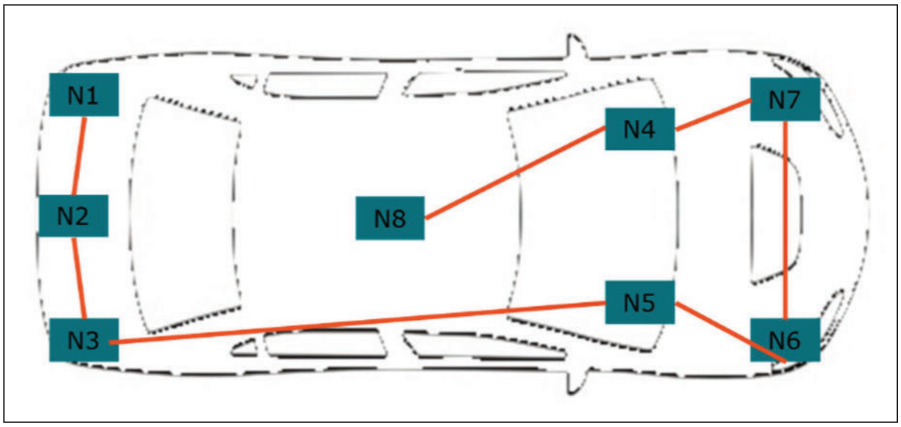

Figure 1: Typical configuration of Ethernet nodes in a modern vehicle

100BASE-T1 and 1000BASE-T1 is based on an unshielded twisted pair (UTP) as shown in Figure 2. UTP cables are widely used in the automotive industry and therefore they are common, easy to use, and economic. However, they have some pitfalls, especially when looking at EMC behavior.

In a modern car, hundreds of meters of cable are connecting all the different electrical units – from a simple climate control unit to a very powerful generator. Those cables are typically put in bundles which increases the risk of electromagnetic interference (EMI) between them. Further investigations have shown that, in worst-case scenarios, EMI can lead to induced peak voltage amplitudes of up to 100 V in the UTP. Considering that this can happen during normal operation when stable data transfer is required, the Ethernet circuitry should be robust enough to withstand those EMC issues.

The circuitry of each node is shown as standardized by the OPEN Alliance (see Figure 3). It includes a common mode choke (CMC) which filters the unwanted common mode noise that couples in the UTP. Additionally, the common mode termination is helpful here. The properties of the CMC for 100BASE-T1 and 1000BASE-T1 are defined in the CMC Test Specifications for these standards[1]. In addition to its filtering and EMC properties, the CMC is also very helpful when it comes to ESD, which we'll address in the next section.

From the perspective of the ESD protection device, there are several very interesting points to consider. First, based on the possible electromagnetic noise on the UTP, the ESD device should not be activated in a voltage range of up to 100 V. Speaking in ESD device parameters, the ESD device is allowed to trigger only above 100 V, as shown in Figure 3 in the TLP graph. Such a high value may sound scary as most of the physical layer (PHY) for high-performance cameras and displays cannot sustain such high voltages. We will see later that this specific configuration of the circuitry (with the CMC) provides solid protection for the PHY.

The second requirement is the 15k V ESD robustness based on a minimum of 1000 discharges.

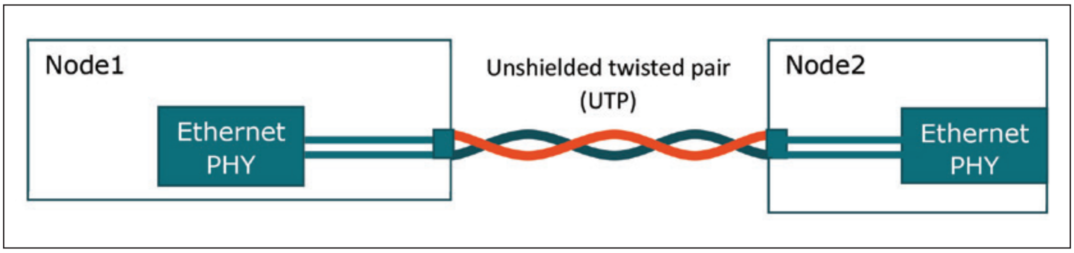

Figure 2: Two Ethernet nodes are connected using an unshielded twisted pair (UTP)

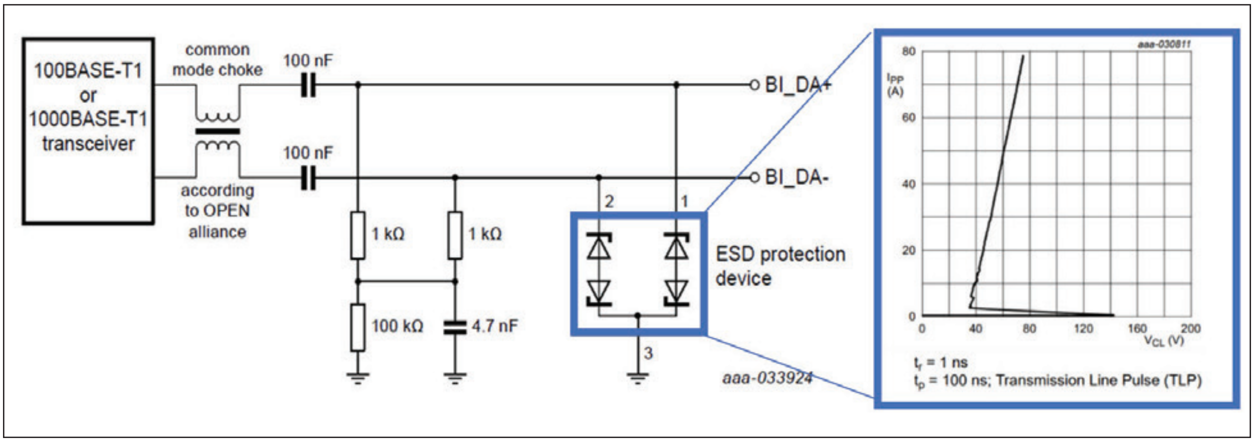

Figure 3: Circuitry of the 100BASE-T1 and 1000BASE-T and the ESD performance of the ESD device

This significant and unique requirement shows the importance of the robust operation of Ethernet-based applications in the automotive environment. All this, combined with the 24 V operation voltage similar to that found in CAN applications, results in a bouquet of special requirements shown in Table 1.

Parameter	Target Value
Working direction	bi-directional
Operation voltage (V_{DCmax})	≥ 24 V
ESD trigger voltage	≥ 100 V
ESD robustness	+/- 15k V contact discharge for unpowered device using discharge module according to ISO 10605 (discharge storage capacitor C = 150 pF and discharge resistor R = 330 Ω
Minimum number of discharges	> 1000
TLP characteristic according to [2]	I/V characteristics

Table 1: Specification of the ESD protections for 100BASE-T1 and 1000BASE-T1[1]

ADDITIONAL ESD TESTING FOR OPEN ALLIANCE ESD PROTECTIONS

In addition to the requirements in Table 1, the ESD device has to withstand additional tests (see Table 2). These tests are usually done by the ESD vendors and can be provided to hardware design engineers.

Test	Purpose
S-Parameters	Signal Integrity
Damage from ESD	Signal integrity after ESD events
ESD Discharge Current	Evaluation of ESD current which flows into the PHY during an ESD event
RF Clamping	Robustness against external EM noise

Table 2: Additional ESD testing for OPEN Alliance standards

The tests for 100BASSE-T1 and 1000BASE-T1 are basically the same but with different pass criteria. The first two tests clearly show the importance of signal integrity (SI) in automotive Ethernet applications. Here, the impact on SI from an ESD protection device should be tested in terms of insertion loss (IL), return loss (RL), and common mode rejection ratio (CMMR) (see Figure 4). For all three parameters, specific limits are given in the "Specification of the ESD protection for 100BASE-T1 and 1000BASE-T1."[1] The ESD discharge current is new in the automotive domain, quantifying the current flowing into the PHY during the ESD event. RF clamping simulates the noise on the UTP covering the 100 V requirement.

PLACEMENT, ROUTING, AND LAYOUT OF THE ESD PROTECTION DEVICES

For a real Ethernet design, the performance of the pure ESD device is not the only important factor. Implementation of the ESD device on the PCB is vital. As already illustrated in Figure 3, the ESD device should be located at the connector. This ensures that the ESD pulse is clamped down to ground directly at the location of the connector, protecting the

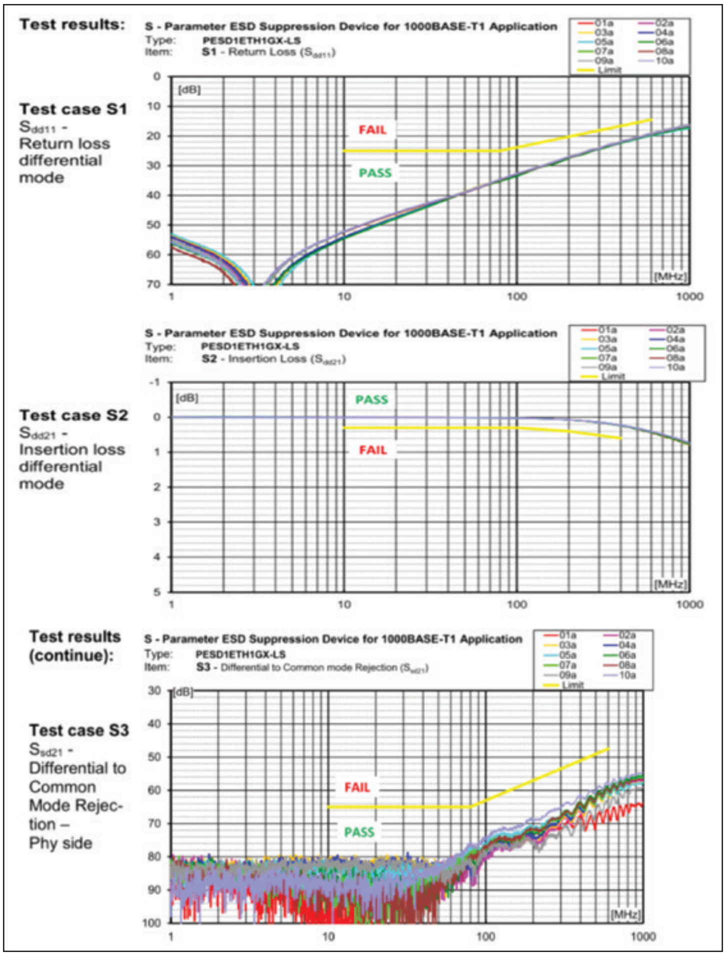

Figure 4: S-parameter results for an ESD protection device for 1000BASE-T1 including the limits in yellow

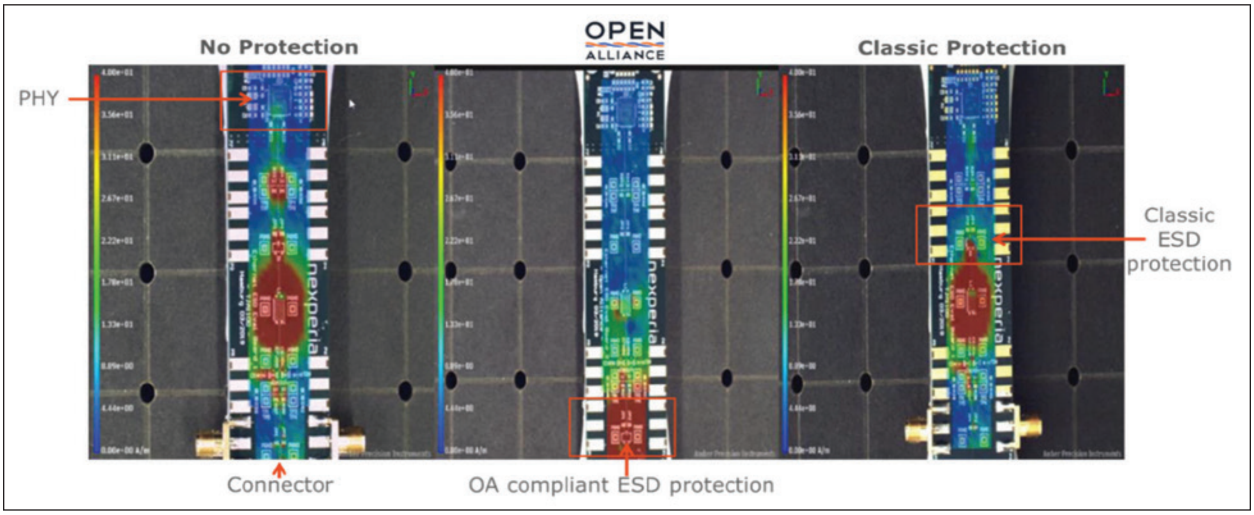

Figure 5: Field scan of the Ethernet circuitry during an ESD event. The red color highlights high current density. For the OA approach, having the ESD device close to the connector gives the lowest current density at the PHY location, and the entire circuitry provides the best ESD performance for the system.

entire circuitry including the CMC, the CMT, and the PHY itself. Figure 5 shows visual proof of how important the placement is.

Here it is crucial to understand that CMC is reducing the ESD stress for the PHY. This is explained when looking at the CMC behavior under pulsed conditions (see Figure 6).

Here the transmission line pulse (TLP) method is used to show that, when a transient pulse (e.g., ESD pulse) is heading to the CMC, it blocks the current for a specific period of time (phase II [the peak in phase I is a measurement artifact]). This blocking phase is dependent on the voltage level of the pulse. The higher the voltage, the shorter the blocking phase. The blocking phase is followed by a saturation phase (phase III). Here, the CMC is acting as an inductor that is driven into saturation by the pulse. Once saturated, it starts to conduct the current and the voltage across the CMC drops.

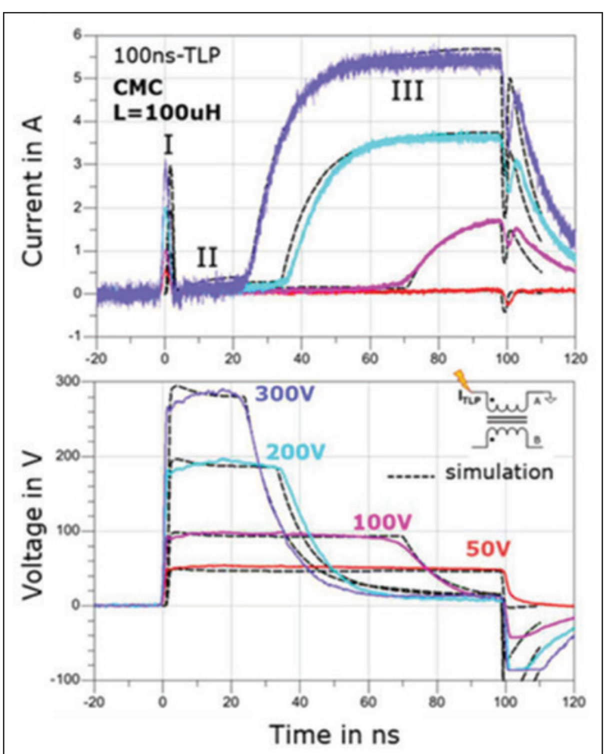

Figure 6: Current and voltage response of a typical CMC for 1000BT1 applications based on TLP measurements. Phase I represents a measuring artifact from TLP. Phase II shows the blocking behavior. Phase III shows the end of the blocking phase and the start of the saturation of the CMC.

As a rule, try to avoid unnecessary layer changes to achieve the best signal integrity. This will always have an impact on the SI and EMC. If changing the layer cannot be avoided, route the signal over the pad of the ESD device

This is an interesting result, as it shows that when an ESD pulse is approaching the 100BASE-T1 or 1000BASE-T1 circuit, the CMC blocks the current for the first several nanoseconds. At the same time, the voltage across the ESD protection device is increasing. Once the trigger level is reached at roughly 140 V (see Figure 3), the ESD device clamps the ESD pulse to ground. The whole voltage on the circuit drops to the clamping voltage of the ESD device which is in the range of 30 to 40 V (see TLP plot in Figure 3).

This finding shows how the combination of a high trigger ESD protection device with a CMC is acting in synergy during ESD events. It should be noted that only CMC with an inductance in the range of ~100μH shows a sufficient blocking behavior, which is covered by the CMC specification anyway.

Typically, ESD protection devices are available in different packages. One that is widely used is the SOT23, a common and established automotive package. An alternative leadless package is the SOD882BD. There are several options for routing the differential lines to and from the package (see Figure 7), with the ranking given in Table 3.

In general, when routing the ESD packages, it should be done straight, avoiding any stubs or bends. Especially for ESD, the traces of differential lines should go over the pad of the ESD device, as it is done for SOT23 [A] and [C] and DFN1006BD (SOD882BD) [A]. For SI purposes, stubs should be avoided and in addition impedance of the differential lines needs to be kept at 100Ω. This can be achieved by keeping the line separated. For SOT23 the best option would be the B and C, and for DFN1006BD it would be option A. So overall, for SOT23 we recommend using option C, and for DFN1006BD option A.

As a rule, try to avoid unnecessary layer changes to achieve the best signal integrity. This will always have an impact on the SI and EMC. If changing the layer cannot be avoided, route the signal over the pad of the ESD device (see Figure 8, left and right). Avoid routing via stubs (see Figure 8, middle).

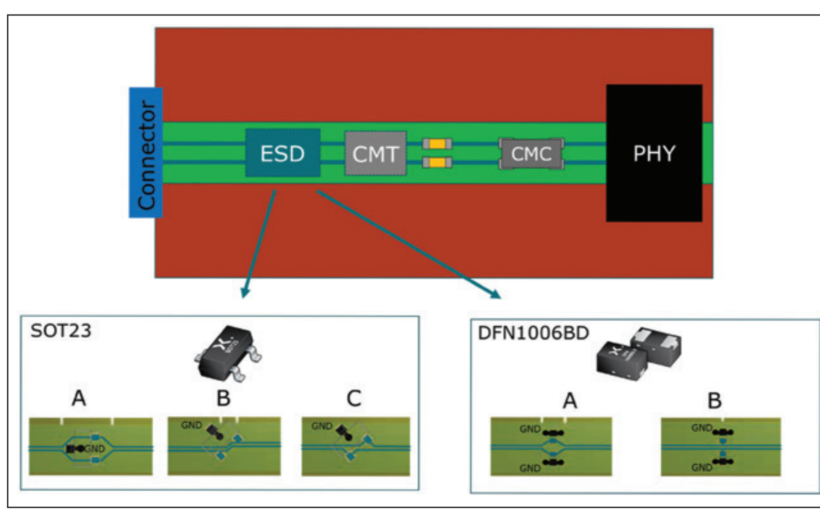

Figure 7: Routing options for SOT23 and SOD882BD

	SOT23			DFN1006BD	
	A	B	C	A	B
Signal Integrity	↓	↑	↑	→	↑
ESD	↑	↓	↑	↑	↓

Table 3: Ranking of the different routing options with regard to ESD and SL

CONCLUSION AND OUTLOOK

The article discusses some of the unique requirements for the entire circuitry and the ESD protection for 1000BASE-T1 and 1000BASE-T1 applications. Showing that the synergy of the ESD protection devices with the blocking capability of the CMC creates a very robust Ethernet system against EMC noise and ESD. By using the EMI scanner, the importance of the position of the ESD protection directly at the connector is highlighted.

It should be mentioned that 10BASE-T1S is an additional standard that is currently in discussion within the OPEN Alliance committees. Since the entire topology of this protocol including UTP and CMC is very similar to 1000BASE-T1 and 1000BASE-T1, the requirements for the high trigger voltage are expected to be the same.

ENDNOTE

1. Available from http://www.opensig.org.

Figure 8: Routing options for changing layers. Try to route over the pad of the ESD device (left, right). Avoid via stubs (middle). Use adjacent ground vias when changing layers.

CALIBRATING SMART BATTERIES WITH IMPEDANCE TRACKING

Enhancing the Intelligence of a Smart Battery with User Practices

Isidor Buchmann is the founder and CEO of Cadex Electronics Inc. For three decades, Buchmann has studied the behavior of rechargeable batteries in practical, everyday applications, and has written award-winning articles including the best-selling book "Batteries in a Portable World," now in its fourth edition. Buchmann can be reached at isidor.buchmann@cadex.com.

By Isidor Buchmann

The smart battery was hailed as an engineering marvel when it was first introduced in 1994 by Intel and Duracell. The heart is the system management bus, or SMBus, that tracks state-of-charge (SoC) and captures performance data. The SMBus also includes the battery management system (BMS) to assure the safe operation of Li-ion batteries by limiting over-voltage and preventing current overloads.

Unlike a regular battery in which the charger is in command, the smart battery is the host that controls the charge function in a Level 2 charger. Being the master enables charging future battery chemistries for which no charge algorithm currently exists. Level 3 is a hybrid charger accommodating batteries with SMBus protocol, as well as regular batteries. Level 3 is the preferred system as the charger charges regular batteries and takes control when SMBus communication fails. Level 1 chargers only supported a single chemistry and have been discontinued.

To maintain SoC accuracy, a smart battery requires periodic calibration. Without the ability to calibrate in the field, the device manufacturer advises a periodic full discharge in the device. The service resets the discharge flag which is followed by a full charge to reset the charge flag as illustrated in Figure 1. Calibration thus establishes a linear line between a full and empty battery to measure SoC. In time, the line will blur again and a recalibration is needed. Device manufacturers advise to calibrate smart batteries every three months or after 40 partial discharges. The need to calibrate is recorded by the Max Error metric. A number 1 reflects a calibrated battery; higher figures indicate the need for service.

A charge-discharge-charge calibration cycle as shown in Figure 1 does not correct loss of capacity. Even though the SoC gauge shows 100%, a fully charged battery with a usable capacity of 50% can only deliver half the specified runtime. As the battery fades, the energy container shrinks, and Figure 2 exemplifies this phenomenon by adding rocks.

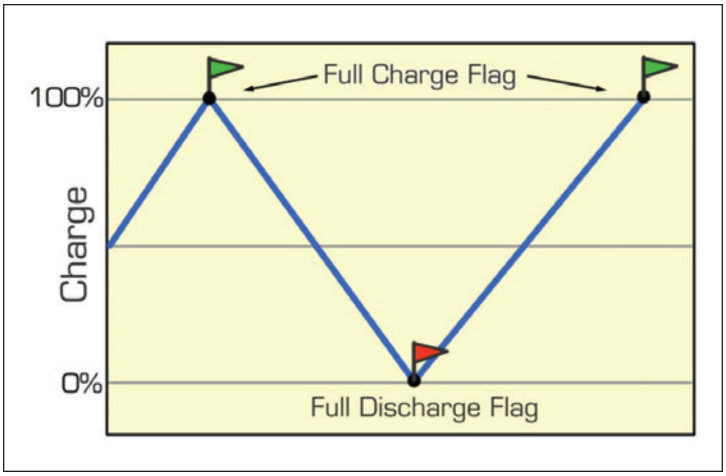

Figure 1: Calibration sets the full charge and empty flags

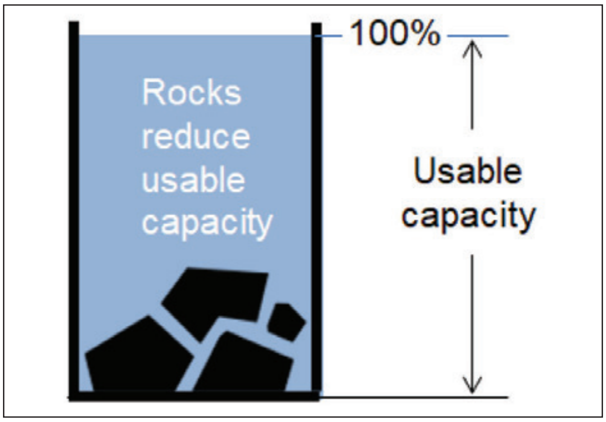

Figure 2: Rocks symbolize capacity loss

The smart battery reveals the usable capacity in full charge capacity. When new, a smart battery's full charge capacity is equal to the design capacity of 100%. However, as the battery fades the percentage of usable capacity drops.

A battery must also have a low internal resistance (Ri) to deliver power. Although capacity loss and rising Ri do not correlate, a definite runtime is only guaranteed if Ri is within specifications. Capacity is the leading health indicator that gradually fades. It's mostly capacity that governs usability and replacement when reaching a low threshold point that is typically 80%.

The smart battery reveals the usable capacity in full charge capacity (FCC). When new, a smart battery's FCC is equal to the design capacity of 100%. However, as the battery fades the percentage of usable capacity drops. Extracted by a smart bus reader, FCC serves as a battery's state-of-health (SoH) indicator.

Testing in our laboratories revealed that, on one-third of smart batteries tested, the correlation error between FCC and usable capacity was greater than 5%. Depending on how a battery is used, the internal fuel gauge tracking FCC can drift out of calibration which will also affect SoC accuracy. Users will experience a battery suddenly dying when it indicated 20% SoC just moments before.

IMPEDANCE TRACKING

In addition to SoC, modern smart batteries feature impedance tracking to assess SoH by counting in-and-outflowing coulomb (the amount of charge delivered by 1A of current in one second). An analogy is a glass holding a liquid content of 20% that is being filled to 100% while measuring the inflowing energy. Residual capacity plus added charge reveals the usable capacity, as Figure 3 illustrates.

Impedance tracking requires assessing the remaining charge (old fill) before recharge. The smart battery does this by measuring the open circuit voltage (OCV), a value that is compared against a reference curve matching the battery chemistry. Because of agitation after a charge and discharge, rest periods are needed to reach voltage equilibrium for SoC estimation. An after-charge needs a minimal rest of two hours; an after-discharge requires a five-hour rest. The system also adds temperature compensation as cold and heat affect the cell voltage.

Despite these precautions, the smart battery loses accuracy and requires occasional calibration. A formal calibration should be done with a battery analyzer to also reset the Max Error because a full cycle does not do this. Battery analyzers also display the usable capacity and Ri to verify SoH.

Before replacement, all batteries should be serviced with a battery analyzer as smart batteries often fail because of digital defects. A calibration may need to be repeated to get the best results. Battery analysis lowers the total cost of ownership and protects

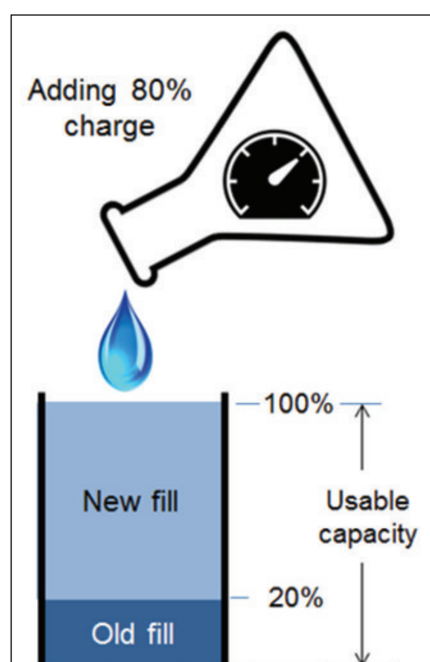

Figure 3: Capacity is the sum of residual charge plus energy added

the environment by helping to increase a battery's anticipated useful life.

CALIBRATING AN EV BATTERY

The BMS in an electric vehicle (EV) works similarly to a portable smart battery, but the driver is relieved of calibration. We ask: "Why does my smart battery need calibration while the EV goes free?" The answer lies in self-calibration that applies to both EV and smart batteries featuring impedance tracking.

Self-calibration utilizes given field opportunities that occur naturally to establish SoC orientation points (SoC-OP) as shown in Figure 4. These points are established when the battery is either charging or discharging and is allowed to reach an equilibrium voltage. Measuring the amount of charge or discharge transferred between two points allows the BMS to update its internal estimate

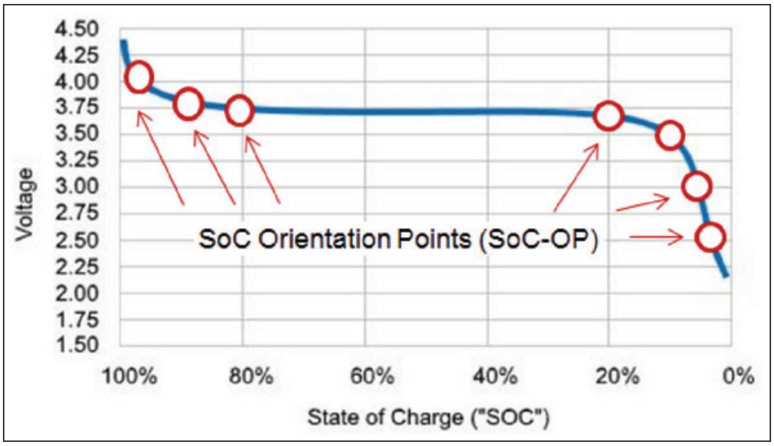

Figure 4: SoC orientation points are set and readjusted with opportunity

The modern smart battery self-calibrates when given the opportunity during a charge or undisturbed discharge if given sufficient rest in between to establish the SoC-OPs.

of capacity. Self-calibration works best when the SoC-Ops are spaced far apart.

A low SoC-OP typically occurs at the end of a day or after a full discharge. A deliberate delay before charging will provide the required rest period to solidify the low SoC-OP; a rest after a full charge sets the high SoC-OP to complete self-calibration. These functions occur naturally during normal use and can be augmented by a thoughtful battery user.

EV batteries use a similar principle, a method that can also be enhanced with clever timing between use and charge by the vehicle owner. Because of the flat discharge curve of a Li-ion battery in the mid-SoC range, the best SoC-OP locations are below 30% and above 70% SoC. The LiFePO (LFP)[1] in the lithium battery family has a very flat midrange curve, but the more popular NMC has a measurable mid-charge tilt. Knowing these characteristics, an EV battery can be calibrated without tools by following this procedure:

1. Apply a deep discharge by driving the extra mile. Be mindful when at a low charge state as the vehicle's indicated range can be off by as much as 30%. Extreme low SoC is noticed when acceleration becomes sluggish. Do not drive further as the battery enters a high-stress mode. The driver can also get stranded.
2. At low SoC, allow the battery to rest for 4 to 6 hours before beginning a charge. Ensure that the car is in deep-sleep mode by disabling all auxiliary loads.
3. After the allotted time, charge the battery to between 80% and 100%. Avoid ultra-fast charging as this causes added stress. Level 1 and 2 EV chargers work well.[2]
4. After charge, allow a 2- to 4-hour rest with no load on the battery. All Li-ion chargers apply a topping charge that will agitate the rest. A deep-sleep rest must have zero current for two hours.

Calibration can improve range prediction by up to 80km (50 miles), but the service may need to be repeated. Some service centers provide formal calibration for given EVs but this is expensive and time-consuming. Battery calibration is recommended once or twice a year and when buying a used EV.

CALIBRATING ENERGY STORAGE SYSTEMS (ESS)

Batteries in energy storage systems (ESS) share similarities with the EV battery in that the installation contains modules of serial and parallel-connected cells managed by a BMS. Most ESSs are monitored by observing cell voltage, load current, and temperature. Voltage and current measurements enable SoC and Ri readings, but capacity assessment to determine the end-of-life on capacity is not attainable. Some ESSs include artificial neural networking[3] by "massaging" big data to assess SoH. Self-calibration with impedance tracking can also be used for ESS applications.

CAN BUS

The SMBus is not the only communication channel for a smart battery. The controller area network (CAN Bus) is a vehicle bus standard that allows the battery to communicate with a host system. Developed by Robert Bosch in 1983, the CAN Bus is primarily used in hybrid vehicles, including e-bikes, drones, and robots.

CELL BALANCING

With thousands of cells connected in series and parallel,[4] a cell imbalance can occur in time. Best cell balancing[5] happens at the battery assembly plant by using quality cells that are tightly matched in capacity. Cell balancing is not as effective as calibration because the weak cells remain weak, even after being fully charged. Cell balancing does not correct a battery pack in the same way calibration does.

CONCLUSION

The modern smart battery self-calibrates when given the opportunity during a charge or undisturbed discharge if given sufficient rest in between to establish the SoC-Ops. The best results are achieved by applying a formal calibration with specified rest periods on a battery analyzer. Periodic calibration is also recommended for the EV. The smart battery is indeed smart but, left under-serviced, the reading can get off by 10 to 20%. Unless regularly calibrated, SoC and FCC data of portable batteries should be taken as reference readings only.

REFERENCES

1. See "BU-205: Types of Lithium Ion," available at https://batteryuniversity.com/article/bu-205-types-of-lithium-ion.
2. See "BU-1004: Charging and Electric Vehicle," available at https://batteryuniversity.com/article/bu-1004-charging-an-electric-vehicle.
3. See "BU-907b: Advancements in Battery Testing," available at https://batteryuniversity.com/article/bu-907b-advancements-in-battery-testing.
4. See "BU-302: Series and Parallel Battery Configurations," available at https://batteryuniversity.com/article/bu-302-series-and-parallel-battery-configurations.
5. See "BU-803a: Cell Matching and Balancing," available at https://batteryuniversity.com/article/bu-803a-cell-matching-and-balancing.

CHINA'S LATEST REGULATION ON 2.4 GHz AND 5 GHz EQUIPMENT

MIIT 2021 No. 129 Updates China's Requirements for Multiple Types of Radio Services

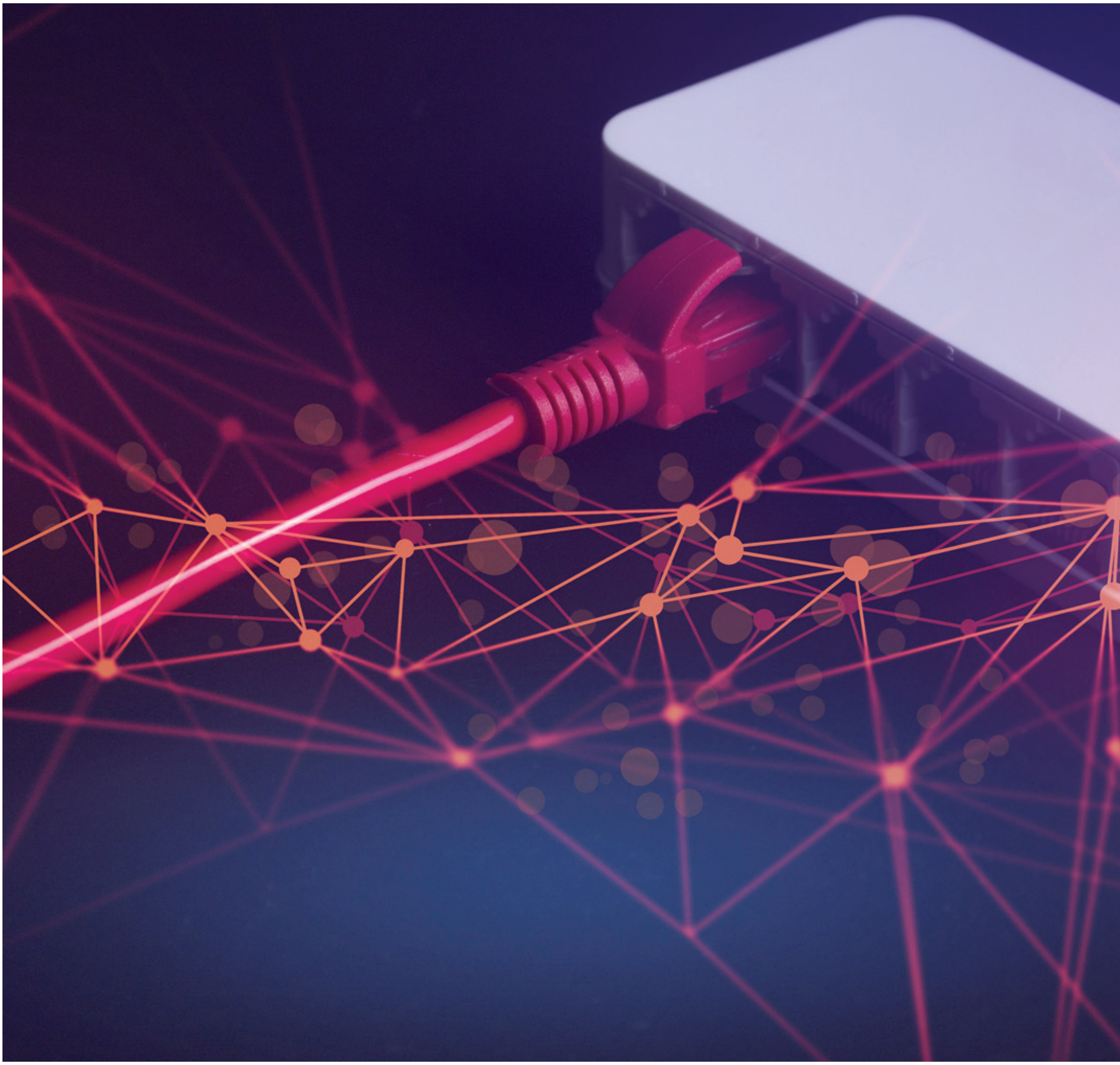

Grace Lin is a Regulatory Compliance Engineer at HYTORC. Prior to joining HYTORC, she was an EMC Staff Engineer and a TCB Reviewer at Intertek. Lin can be reached at glin@hytorc.com.

By Grace Lin

On October 13, 2021, the Ministry of Industry and Information Technology of the People's Republic of China (MIIT) issued MIIT 2021 No. 129, "Notice on Strengthening and Standardizing the Radio Management of 2400 MHz, 5100 MHz, and 5800 MHz bands." This regulation came into effect on January 1, 2022, with a two-year transitional period.

SCOPE

MIIT 2021 No. 129 applies to equipment operating in the 2400-2483.5 MHz, 5150-5350 MHz, and 5725-5850 MHz frequency bands which are allocated for multiple types of radio services, including fixed, mobile, radio navigation, fixed-satellite, earth exploration-satellite, satellite radiolocation, or space research applications. The 2400-2483.5 MHz and 5725-5850 MHz bands are also designated for industrial, scientific, and medical (ISM) applications that emit electromagnetic energy, which is subject to a different regulation. Radio stations or equipment do not have exclusive access to or use of the 2400-2483.5 MHz, 5150-5350 MHz, and 5725-5850 MHz frequency bands.

The 2400-2483.5 MHz frequency band can be used for radio communications systems utilizing wideband radio access (including wireless local area network (LAN)), Bluetooth transceivers, and point-to-point transmission. The 5150-5350 MHz frequency band can be used for radio communications systems utilizing wideband radio access (including wireless LAN), but is restricted to indoor use only (except devices installed in vehicles). The 5725-5850 MHz frequency band can be used for radio communication systems utilizing wideband radio access (including wireless LAN), point-to-point transmission, and electronic toll collections (ETC).

TECHNICAL REQUIREMENTS

General Technical Requirements

The general technical requirements under MIIT 2021 No. 129 are summarized in Table 1 on page 36. Antenna assembly gain and beamforming gain are taken into account for equipment employing multiple antennas, when performing equivalent isotropically radiated power (EIRP, $P_{e.i.r.p.}$) and power spectrum density ($PSD_{e.i.r.p.}$) measurements.

Radio equipment operating in the 5250-5350 MHz frequency band must incorporate transmit power control (TPC) and dynamic frequency selection (DFS) functions and shall not include any feature designed to turn off the DFS function. TPC is a feature that enables a device to dynamically switch between several transmission power levels in the data transmission process. For equipment without TPC function, limits of $P_{e.i.r.p}$ and $PSD_{e.i.r.p.}$ shall be 3 dB lower. DFS is a mechanism that dynamically detects signals from other systems and avoids co-channel operation with these systems.

Wireless LAN equipment with public network IP address allocation function shall support IPv6 protocol and enable the IPv6 address allocation function by default.

Adaptivity

Adaptivity is an automatic channel access mechanism by which a device limits its transmissions and gains access to an operating channel. It is intended to detect transmissions from other wireless LAN devices operating in the band. To comply with the requirements of MIIT 2021 No. 129, equipment operating in the 2400-2483.5 MHz, 5150-5350 MHz, and 5725-5850 MHz frequency bands shall implement an adaptivity mechanism. Adaptivity requirements

Parameter	Limits / Specifications		
Frequency Band (MHz)	2400-2483.5	5150 - 5350	5725 – 5850
EIRP Power, $P_{e.i.r.p}$	Antenna Assembly Gain < 10 dBi: ≤ 20 dBm Antenna Assembly Gain ≥ 10 dBi: ≤ 27 dBm	≤ 23 dBm	≤ 33 dBm
EIRP Power Spectral Density, $PSD_{e.i.r.p}$	1. DSSS or other Equipment: Antenna Assembly Gain < 10 dBi: ≤ 10 dBm/MHz Antenna Assembly Gain ≥ 10 dBi: ≤ 17 dBm/MHz 2. FHSS Equipment: ≤ 20 dBm/100kHz	≤ 10 dBm/MHz	≤ 19 dBm/MHz
Frequency Tolerance	≤ 20 x 10^{-6}	≤ 20 x 10^{-6}	≤ 20 x 10^{-6}
Out of Band Transmit Power	≤ -80 dBm/Hz	≤ -80 dBm/Hz	≤ -80 dBm/Hz
Spurious Emissions [1]	30 MHz – 1 GHz: -36 dBm[2] 1 – 12.75 GHz: -30 dBm[3]	30 MHz – 1 GHz: -36 dBm[2] 1 – 26 GHz: -30 dBm[3]	30 MHz – 1 GHz: -36 dBm[2] 1 – 26 GHz: -30 dBm[3]
Spurious Emissions [1] - Special Bands	48.5 – 72.5 MHz: -54 dBm[2] 76 – 118 MHz: -54 dBm[2] 167 – 223 MHz: -54 dBm[2] 470 – 702 MHz: -54 dBm[2] 2300 – 2380 MHz: -40 dBm[3] 2380 – 2390 MHz: -40 dBm[2] 2390 – 2400 MHz: -30 dBm[2] 2400 – 2483.5 MHz *: -33 dBm[2] 2483.5 – 2500 MHz: -40 dBm[3] 5150 – 5350 MHz: -40 dBm[3] 5725 – 5850 MHz: -40 dBm[3]	48.5 – 72.5 MHz: -54 dBm[2] 76 – 118 MHz: -54 dBm[2] 167 – 223 MHz: -54 dBm[2] 470 – 702 MHz: -54 dBm[2] 2400 – 2483.5 MHz: -40 dBm[3] 2483.5 – 2500 MHz: -40 dBm[3] 5150 – 5350 MHz *: -33 dBm[2] 5725 – 5850 MHz: -40 dBm[3]	48.5 – 72.5 MHz: -54 dBm[2] 76 – 118 MHz: -54 dBm[2] 167 – 223 MHz: -54 dBm[2] 470 – 702 MHz: -54 dBm[2] 2400 – 2483.5 MHz: -40 dBm[3] 2483.5 – 2500 MHz: -40 dBm[3] 5150 – 5350 MHz: -40 dBm[3] 5470 – 5705 MHz: -40 dBm[3] 5705 – 5715 MHz: -40 dBm[2] 5715 – 5725 MHz: -30 dBm[2] 5725 – 5850 MHz *: -33 dBm[2] 5850 – 5855 MHz: -30 dBm[2] 5855 – 7125 MHz: -40 dBm[3]
Dynamic Frequency Selection (DFS) (5250-5350 MHz only)	Not applicable	1. Detection Threshold: ≤ -62 dBm, 2. Detection Probability: ≥ 60%, 3. Channel Availability Check Time: ≥ 60 s, 4. Channel Move Time: ≤ 10 s, 5. Channel Close Transmit Time: ≤ 1 s, 6. Non-occupancy Period: ≥ 30 min	Not applicable
Transmit Power Control (TPC) (5250-5350 MHz only)	Not applicable	≥ 6 dB	Not applicable

1. Detection = RMS.
2. RBW = 100 kHz
3. RBW = 1 MHz

*: In band spurious emissions

DSSS: Direct Sequence Spread Spectrum
EIRP: Equivalent Isotropically Radiated Power
FHSS: Frequency Hopping Spread Spectrum
RBW: Resolution Bandwidth

Table 1: General technical requirements

Channel Access Mechanism	Listen Before Talk (LBT)			Detect And Avoid (DAA)	
Equipment Type	FHSS	Non-FHSS		FHSS	Non-FHSS
		Frame Based Equipment	Load Based Equipment		
CCA Observation Time	≥0.2% COT; ≥16 µs	≥16 µs	≥16 µs	-	-
Silent Period	-	-	-	1 s or 5 x Hopping Frequencies x COT, whichever is greater	1 s
Duty Cycle of SCST	≤10%	≤10%	≤10%	≤10%	-
Channel Occupancy Time (COT)	<60 ms	1 ms ≤ COT ≤ 10 ms	≤13 ms	≤40 ms	≤40 ms
Idle Period	≥5% COT; ≥100 µs	≥5% COT	-	≥5% COT; ≥100 µs	≥5% COT; ≥100 µs
Detection Threshold Level (TL)	TL ≤ -70 dBm/MHz + 10 × lg (100 mW / P_{out}) P_{out}: EIRP Power in mW				
Unwanted Signal Parameters	2395 MHz or 2488.5 MHz: -35 dBm, Continuous Wave (CW)				

CCA: Clear Channel Assessment

FHSS: Frequency Hopping Spread Spectrum

SCST: Short Control Signaling Transmissions

Table 2: Adaptivity parameters and required specifications (2400-2483.5 MHz)

are similar to the requirements in ETSI EN 300 328 (2400-2483.5 MHz frequency band) and ETSI EN 301 893 (5150-5350 MHz, and 5725-5850 MHz frequency bands).

Equipment operating in the 2400-2483.5 MHz frequency band shall implement either a "Listen Before Talk" (LBT) or a "Detect And Avoid" (DAA)-based channel access mechanism. Adaptivity parameters and specifications for this frequency band are summarized in Table 2.

Equipment operating in the 5150-5350 MHz and 5725-5850 MHz frequency bands shall implement an LBT-based channel access mechanism. Adaptivity parameters and specifications for these frequency bands are summarized in Table 3 on page 38.

For equipment operating in the 2400-2483.5 MHz frequency band, and not supporting any one of the above adaptivity mechanisms, and for the electronic toll collections (ETC) equipment operating in the 5725-5850 MHz frequency band, an "equivalent usage rate" mechanism applies. "Equivalent usage rate" (EU) shall not be greater than 10%, as calculated by using the following formula:

$$EU = \left(\frac{P_{e.i.r.p}(mW)}{P_{limit}(mW)} \right) \times DC$$

Where EU is the equivalent usage rate, DC is the duty cycle, and P_{limit} is EIRP power limit.

Effective October 15, 2023, equipment that falls under the scope of this regulation must comply with the technical requirements stipulated in MIIT 2021 No. 129.

EQUIPMENT AUTHORIZATION PROCEDURE

Equipment authorization procedure "Radio Transmission Equipment Type Approval" applies to equipment operating in the 2400-2483.5 MHz, 5150-5350 MHz, and 5725-5850 MHz frequency bands, except for low-power short range devices (SRDs) and ISM equipment. All certified equipment is listed on the MIIT online service platform at https://ythzxfw.miit.gov.cn/resultQuery.

Regulations for the low power SRDs and ISM equipment are stipulated in China MIIT 2019 No. 52. Type approval is not required, but certain statements must be included in the user manual accompanying the equipment. Required technical parameters for the low-power short-range devices (SRDs) and ISM equipment operating in the 2400-2483.5 MHz and 5725-5850 MHz are listed in Table 4 for reference.

TRANSITION

The requirements of MIIT 2021 No. 129 came into effect January 1, 2022, with a transitional period until October 15, 2023. The Regulation supersedes previous issued relevant regulations including, but not limited to, the following four regulations:

1. "Notice on Adjusting 2.4 GHz Frequency Band Transmit Power Limits and Relevant Matters"
2. "Notice on the Use of 5.8 GHz Frequency Band"
3. "Notice on the Special Use of Intelligent Traffic Management of 5.8 GHz Frequency Band Wireless Short Range Communication Systems and Relevant Matters"
4. "Notice on Use of 5150-5350 MHz Frequency Band Wireless Access Systems and Relevant Matters"

Effective October 15, 2023, equipment that falls under the scope of this regulation must comply with the technical requirements stipulated in MIIT 2021 No. 129. Prior to October 15, 2023, equipment may comply with technical requirements stipulated in the precedent regulations. Certificates applicable to equipment complying with the precedent regulations and certified after January 1, 2022 will expire on December 31, 2025.

CONCLUSION

Technical requirements from China MIIT 2021 No. 129 are significantly different from their precedent regulations. Complying with adaptivity, DFS, and TPS is now required. Spurious emissions limits apply to additional frequency bands. An EU

Channel Access Mechanism	Listen Before Talk (LBT)	
Equipment Type	Frame Based Equipment	Load Based Equipment
Fixed Frame Periods (FFP)	1ms ≤ FFP ≤ 10ms	-
CCA Observation Time	≥16 µs	≥25 µs
Channel Occupancy Time (COT)	≤95% FFP	≤20 ms
Idle Period	≥5% COT, ≥100µs	-
SCST Transmissions	≤50 within 50 ms	≤50 within 50 ms
Total SCST Transmissions Duration	2500 µs	2500 µs
Duty Cycle of SCST	≤10%	≤10%
Detection Threshold Level (TL)	≤-75 dBm/MHz	

CCA: Clear Channel Assessment

SCST: Short Control Signaling Transmission

Table 3: Adaptivity parameters and required specifications (5150-5350 MHz and 5725-5850 MHz)

Parameter	Limits / Specifications	
Frequency Band (MHz)	2400-2483.5	5725 – 5850
EIRP Power, $P_{e.i.r.p}$	10 mW	25 mW
Frequency Tolerance	75 kHz	100×10^{-6}

Table 4: Technical requirements for the low-power SRDs and ISM equipment

rate adaptivity mechanism is introduced. Addressing these new technical requirements at the early stage of product development will help shorten the overall design cycle and speed up the introduction of new products to China's market.

ACKNOWLEDGMENTS

The author would like to thank Jessy Zhang of G&M Compliance for providing relevant information regarding China MIIT 2021 No. 129.

The author wishes to express her sincere appreciation to Wayne Owens of HYTORC for his support.

REFERENCES

- "Notice on Strengthening and Standardizing the Radio Management of 2400 MHz, 5100 MHz, and 5800 MHz bands," China MIIT 2021 No. 129, issued October 13, 2021. https://wap.miit.gov.cn/zwgk/zcwj/wjfb/tz/art/2021/art_e4ae71252eab42928daf0ea620976e4e.html
- Interpretation on "Notice on Strengthening and Standardizing the Radio Management of 2400 MHz, 5100 MHz, and 5800 MHz bands," issued October 14, 2021. https://wap.miit.gov.cn/zwgk/zcjd/art/2021/art_f9d24f82c2b24a16b357ae883f21a65e.html
- "Low Power Short Range Devices Regulations," China MIIT 2019 No. 52. https://www.miit.gov.cn/jgsj/wgj/wjfb/art/2020/art_792ab84586c34b64bb391eb6496c0953.html
- "Low Power Short Range Devices Categories and Technical Requirements," China MIIT 2019 No. 52 Attachment. https://www.miit.gov.cn/cms_files/filemanager/oldfile/miit/n1146285/n1146352/n3054355/n3057735/n3057748/n8004149/c8006552/part/8006563.pdf
- "Notice on the Use of 5.8 GHz Frequency Band," China MIIT 2002 No. 277, issued September 5, 2009. http://www.srrc.org.cn/article1362.aspx
- "Notice on Adjusting 2.4 GHz Frequency Band Transmit Power Limits and Related Matters," China MIIT 2002 No. 353, issued May 30, 2019. https://ahca.miit.gov.cn/wzpz/xwtt/art/2020/art_a34aec22d220441e90db0a66870bcaf8.html
- "Notice on the Use of 5150-5350 MHz Frequency Band Wireless Access Systems and Related Matters," China MIIT 2012 No. 620, issued January 30, 2013.
- "Notice on the Special Use of Intelligent Traffic Management of 5.8 GHz Frequency Band Wireless Short Range Communication Systems and Related Matters," China MIIT 2003 No. 225.
- "Wideband transmission systems; Data transmission equipment operating in the 2,4 GHz band; Harmonised Standard for access to radio spectrum," ETSI EN 300 328 V2.2.2 (2019-07). https://www.etsi.org/deliver/etsi_en/300300_300399/300328/02.02.02_60/en_300328v020202p.pdf
- "5 GHz RLAN; Harmonised Standard covering the essential requirements of article 3.2 of Directive 2014/53/EU," ETSI EN 301 893 V2.1.1 (2017-05). https://www.etsi.org/deliver/etsi_en/301800_301899/301893/02.01.01_60/en_301893v020101p.pdf

CONCEPT OF A PHASOR IN SINUSOIDAL STEADY STATE ANALYSIS

By Bogdan Adamczyk

This article introduces a concept of a phasor which is extensively used in several EMC topics including electromagnetic waves, antennas, and transmission lines. The following series of articles will use phasors to determine voltages and currents along the transmission line, and subsequently the input impedance to transmission line.

1. SINUSOIDAL VOLTAGES

Consider a single frequency sinusoidal signal

$$v(t) = V\,cos\,\omega\,t \tag{1.1}$$

where *V* is the amplitude of the sinusoid and ω is the angular frequency in radians per second, *rad/s*. The period *T* and the angular frequency ω are related by

$$T = \frac{\omega}{2\pi} \tag{1.2}$$

The reciprocal of the period is the (cyclic) frequency (in Hz)

$$f = \frac{1}{T} \tag{1.3}$$

The angular frequency ω and the cyclic frequency *f* are obviously related by

$$\omega = 2\pi f \tag{1.4}$$

Let us now consider a more general expression for a sinusoid,

$$v(t) = V\,cos(\omega t + \varphi) \tag{1.5}$$

where $(\omega t + \phi)$ is called the argument of the cosine function, and ϕ is its phase.

The sinusoidal functions may, in general, be expressed in any of the four different forms: either as a sine or a cosine function, with either positive or negative "amplitude" [1].

Dr. Bogdan Adamczyk is professor and director of the EMC Center at Grand Valley State University (http://www.gvsu.edu/emccenter) where he regularly teaches EMC certificate courses for industry. He is an iNARTE certified EMC Master Design Engineer. Prof. Adamczyk is the author of the textbook "Foundations of Electromagnetic Compatibility with Practical Applications" (Wiley, 2017) and the upcoming textbook "Principles of Electromagnetic Compatibility with Laboratory Exercises" (Wiley 2022). He can be reached at adamczyb@gvsu.edu.

For example,

$$v_1(t) = 2\,cos(\omega t + 30^\circ) \tag{1.6a}$$

$$v_2(t) = -3\,cos(\omega t - 60^\circ) \tag{1.6b}$$

$$v_3(t) = 4\,sin(\omega t + 45^\circ) \tag{1.6c}$$

$$v_4(t) = -5\,sin(\omega t - 15^\circ) \tag{1.6d}$$

As we will see in the next section, we often need the sinusoid to be expressed as a cosine function with positive amplitude, as shown in Eq. (1.6a). Therefore, we need to be able to transform the other three forms into the positive cosine form. To accomplish that, we could use the following trigonometric identities:

$$-\,cos(\omega t + \theta) = cos(\omega t + \theta \pm 180^\circ) \tag{1.7a}$$

$$sin(\omega t + \theta) = cos(\omega t + \theta - 90^\circ) \tag{1.7b}$$

$$-\,sin(\omega t + \theta) = cos(\omega t + \theta + 90^\circ) \tag{1.7c}$$

Therefore, Eqns. (1.6b-d) can be expressed as

$$v_2(t) = -3\,cos(\omega t - 60^\circ) = 3\,cos(\omega t + 120^\circ) \tag{1.8a}$$

$$v_3(t) = 4\,sin(\omega t + 45^\circ) = 4\,cos(\omega t - 45^\circ) \tag{1.8b}$$

$$v_4(t) = -5\,sin(\omega t - 15^\circ) = 5\,cos(\omega t + 75^\circ) \tag{1.8c}$$

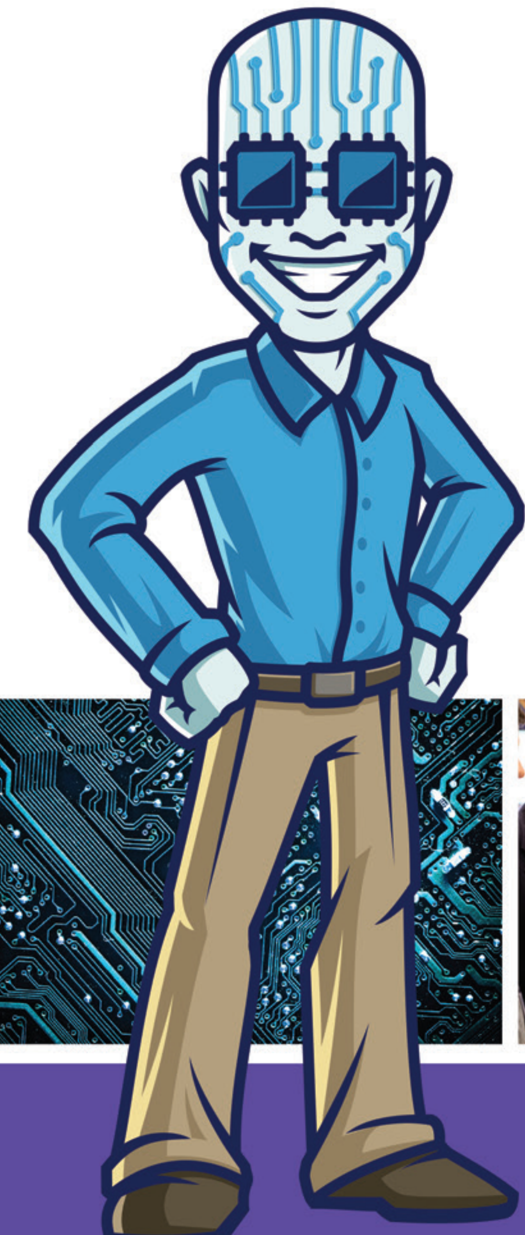

Alternatively, we may use the graphical approach [2], as follows. Consider the set of axis shown in Figure 1. The horizontal axis represents the cosine, while the vertical axis (pointing down) denotes the sine. Angles are measured positively counterclockwise from the horizontal, as in polar coordinates.

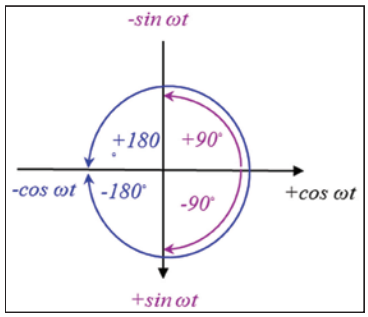

Figure 1: Trigonometric relations

This figure can be used to obtain a positive cosine out of the other three forms, as follows. Negative cosine is equivalent to positive cosine plus or minus 180°. Positive sine is equivalent to positive cosine minus 90°. Negative sine is equivalent to positive cosine plus 90°.

2. SINUSOIDS AND PHASORS

Consider a positive cosine function of the form

$$v(t) = V\cos(\omega t + \theta) \tag{2.1}$$

We could use its amplitude and phase to create a related complex number

$$V\angle\theta = Ve^{j\theta} \tag{2.2}$$

Obviously, the complex number in expression (2.2) is *related* to the sinusoid in expression (2.1). We often say that this complex number *represents* the respective sinusoid.

Is this representation useful? Extremely! Instead of performing mathematical operations on sinusoids in time domain (which is often difficult to do), we can perform the operations on complex numbers, related to these sinusoids, in complex domain (which is relatively easy to do).

Note that the sinusoid exists in time domain, while the complex number representing it exists in complex domain. Therefore, they are *not* equal; they *correspond* to each other.

$$V\cos(\omega t + \theta) \leftrightarrow Ve^{j\theta} \tag{2.3}$$

When a complex number represents a sinusoid we call it a *phasor*. By representing the sinusoid as a phasor we transform the sinusoid from the time domain to the phasor or frequency domain.

So what is the difference between a phasor and a complex number? Every phasor is a complex number, but not every complex number is a phasor. Only when the complex number represents a sinusoid, it is referred to as a phasor.

In electromagnetic compatibility we often deal with complex voltages and currents. These complex expressions represent sinusoids in time domain, and therefore are phasors. We also encounter complex impedance, but the impedance does not represent a time-domain sinusoid; therefore, it is not a phasor, it is just a complex expression.

To distinguish between the time domain variables and the complex variables, we will adopt the notation from [3]. Complex variable will always have a "hat" above it.

$$\hat{V} = V\angle\theta = Ve^{j\theta} \tag{2.4}$$

In the above expression, the magnitude V and the angle θ are real, thus do not have "hats" but the phasor is complex.

Given a phasor, in polar or exponential form, we can easily determine the time-domain sinusoid corresponding to it. For instance, if the phasor is given by

$$\hat{I} = Ie^{j\theta} \tag{2.5}$$

then the sinusoid corresponding to it, simply is

$$\hat{I} = Ie^{j\theta} \Leftrightarrow i(t) = I\cos(\omega t + \theta) \tag{2.6}$$

Alternatively, the time-domain form of phasor quantities may be obtained by multiplying the phasor form by $e^{j\omega t}$ and taking the real part of the result.

$$Re\left\{\hat{I}e^{j\omega t}\right\} = I\cos(\omega t + \theta) = i(t) \tag{2.7}$$

3. DERIVATIVE IN PHASOR DOMAIN

Let the time-domain sinusoid be expressed as

$$v(t) = V\cos(\omega t + \theta) \tag{3.1}$$

Its corresponding phasor is

$$\hat{V} = Ve^{j\theta} \tag{3.2}$$

If we take the derivative of *v(t)* in expression (3.1) we will obtain another sinusoid; a negative sine function, to be exact. That negative sine function can be expressed as a positive cosine using the transformations discussed earlier.

Therefore, we could create a phasor representing it. The question we pose is as follows: what is the relationship between the original phasor representing *v(t)* and the phasor representing its derivative?

To answer this question let us take the derivative of *v(t)*:

$$\frac{dv(t)}{dt} = -\omega V \sin(\omega t + \theta) = \omega V \cos(\omega t + \theta + 90°) \tag{3.3}$$

Thus, the phasor representing the derivative of *v(t)* is

$$\omega V \cos(\omega t + \theta + 90°) \leftrightarrow \omega V e^{j(\theta + 90°)} \tag{3.4}$$

Let's have a closer look at this phasor.

$$\omega V e^{j(\theta + 90°)} = \omega V e^{j\theta} e^{j90°} \tag{3.5}$$

However,

$$e^{j90°} = \cos 90° + j \sin 90° = j \tag{3.6}$$

and therefore

$$\omega V e^{j\theta} e^{j90°} = j\omega V e^{j\theta} = j\omega \hat{V} \tag{3.7}$$

We arrived at a very important observation.

$$v(t) \leftrightarrow \hat{V} \tag{3.8a}$$

$$\frac{dv(t)}{dt} \leftrightarrow j\omega \hat{V} \tag{3.8b}$$

That is, to obtain the phasor representing the derivative of a (sinusoidal) function, we simply take the phasor representing that function and multiply it by *jω*. What about the phasor representing the second derivative? We simply multiply the phasor representing the first derivative by another *jω* term.

$$\frac{d^2v(t)}{dt^2} \leftrightarrow j\omega\left(j\omega\hat{V}\right) = -\omega^2\hat{V} \tag{3.8c}$$

4. EMC APPLICATIONS

4.1 Electromagnetic Fields

Of major interest in EMC are the sinusoidal electromagnetic fields with the time-domain vectors and scalar expressions being the sinusoidal functions of time and space.

For instance, the electric field intensity vector ***E*** in time domain is given by

$$\boldsymbol{E}(x,y,z,t) = \left[E_x(x,y,z,t), E_y(x,y,z,t), E_z(x,y,z,t)\right] \tag{4.1}$$

where each of its components is a sinusoidal function

$$E_x(x,y,z,t) = E_{xm}\cos(\omega t + \theta_{xE}) \tag{4.2a}$$

$$E_y(x,y,z,t) = E_{ym}\cos(\omega t + \theta_{yE}) \tag{4.2b}$$

$$E_z(x,y,z,t) = E_{zm}\cos(\omega t + \theta_{zE}) \tag{4.2c}$$

The corresponding phasors are

$$\hat{E}_x(x,y,z) = E_{xm}\angle\theta_{xE} = E_{xm}e^{j\theta_{xE}} \tag{4.3a}$$

$$\hat{E}_y(x,y,z) = E_{ym}\angle\theta_{yE} = E_{ym}e^{j\theta_{yE}} \tag{4.3b}$$

$$\hat{E}_z(x,y,z) = E_{zm}\angle\theta_{zE} = E_{zm}e^{j\theta_{zE}} \tag{4.3c}$$

Thus, the phasor form of the ***E*** vector in Eq. (4.1) is

$$\hat{\boldsymbol{E}}(x,y,z) = \left[\hat{E}_x(x,y,z), \hat{E}_y(x,y,z), \hat{E}_z(x,y,z)\right] \tag{4.4}$$

Similarly, if the magnetic field intensity vector ***H*** in time domain is given by

$$\boldsymbol{H}(x,y,z,t) = \left[H_x(x,y,z,t), H_y(x,y,z,t), H_z(x,y,z,t)\right] \tag{4.5}$$

with each of its components being a sinusoidal function

$$H_x(x,y,z,t) = H_{xm}\cos(\omega t + \theta_{xH}) \tag{4.6a}$$

$$H_y(x,y,z,t) = H_{ym}\cos(\omega t + \theta_{yH}) \tag{4.6b}$$

$$H_z(x,y,z,t) = H_{zm}\cos(\omega t + \theta_{zH}) \tag{4.6c}$$

Then the corresponding phasors are

$$\hat{H}_x(x,y,z) = H_{xm}\angle\theta_{xH} = H_{xm}e^{j\theta_{xH}} \tag{4.7a}$$

$$\hat{H}_y(x,y,z) = H_{ym}\angle\theta_{yH} = H_{ym}e^{j\theta_{yH}} \tag{4.7b}$$

$$\hat{H}_z(x,y,z) = H_{zm}\angle\theta_{zH} = H_{zm}e^{j\theta_{zH}} \tag{4.7c}$$

Thus, the phasor form of the $\boldsymbol{H}$ vector in Eq. (4.5) is

$$\hat{\boldsymbol{H}}(x,y,z) = \left[\hat{H}_x(x,y,z), \hat{H}_y(x,y,z), \hat{H}_z(x,y,z)\right] \tag{4.8}$$

4.2 Maxwell's Equations

Maxwell's equations can be expressed in several forms. Here, we present the differential, time-domain version of these equations in simple medium [1,3].

$$\nabla \times \boldsymbol{E} = -\mu\frac{\partial \boldsymbol{H}}{\partial t} \tag{4.9a}$$

$$\nabla \times \boldsymbol{H} = \sigma\boldsymbol{E} + \varepsilon\frac{\partial \boldsymbol{E}}{\partial t} + \boldsymbol{J}_S \tag{4.9b}$$

$$\nabla \cdot \boldsymbol{E} = \frac{\rho_V}{\varepsilon} \tag{4.9c}$$

$$\nabla \cdot \boldsymbol{H} = 0 \tag{4.9d}$$

In Eqns. (4.9) $\boldsymbol{E}$ denotes electric field intensity, while $\boldsymbol{H}$ denotes magnetic field intensity. $\boldsymbol{J}$ stands for volume current density, while ρ_v denotes volume charge density.

The corresponding phasor-domain equations are

$$\nabla \times \hat{\boldsymbol{E}} = -j\omega\mu\hat{\boldsymbol{H}} \tag{4.10a}$$

$$\nabla \times \hat{\boldsymbol{H}} = (\sigma + j\omega\varepsilon)\hat{\boldsymbol{E}} + \hat{\boldsymbol{J}}_S \tag{4.10b}$$

$$\nabla \cdot \hat{\boldsymbol{E}} = \frac{\hat{\rho}_V}{\varepsilon} \tag{4.10c}$$

$$\nabla \cdot \hat{\boldsymbol{H}} = 0 \tag{4.10d}$$

4.3 Transmission Line Equations

In time domain, the transmission line equations can be expressed either as a a set of coupled first order equations or a set of uncoupled second order equations. The coupled equations for a lossless line are, [1]:

$$\frac{\partial V(z,t)}{\partial z} = -l\frac{\partial I(z,t)}{\partial t} \tag{4.11a}$$

$$\frac{\partial I(z,t)}{\partial z} = -c\frac{\partial V(z,t)}{\partial t} \tag{4.11b}$$

In Eqns. (4.11) l and c denote inductance and capacitance per unit length, respectively.

The corresponding phasor equations are

$$\frac{d\hat{V}(z)}{dz} = -j\omega l\hat{I}(z) \tag{4.12a}$$

$$\frac{d\hat{I}(z)}{dz} = -j\omega c\hat{V}(z) \tag{4.12b}$$

The uncoupled equations for a lossy line are, [1]:

$$\frac{\partial^2 V(z,t)}{\partial z^2} = lc\frac{\partial^2 V(z,t)}{\partial t^2} + (lg + rc)\frac{\partial V(z,t)}{\partial t} + rgV(z,t) \tag{4.13a}$$

$$\frac{\partial^2 I(z,t)}{\partial z^2} = lc\frac{\partial^2 I(z,t)}{\partial t^2} + (lg + rc)\frac{\partial I(z,t)}{\partial t} + rgI(z,t) \tag{4.13b}$$

In Eqns. (4.13) r and g denote resistance and conductance per unit length, respectively.

The corresponding phasor equations are

$$\frac{d^2\hat{V}(z)}{dz^2} = \hat{\gamma}^2\hat{V}(z) \tag{4.14a}$$

$$\frac{d^2\hat{I}(z)}{dz^2} = \hat{\gamma}^2\hat{I}(z) \tag{4.14b}$$

where $\hat{\gamma}$ is the propagation constant of the line, defined by

$$\hat{\gamma} = \sqrt{(r + j\omega l)(g + j\omega c)} \tag{4.15}$$

REFERENCES

1. Adamczyk, B., *Foundations of Electromagnetic Compatibility with Practical Applications*, Wiley, 2017.
2. Alexander, C. and Sadiku, M., *Fundamentals of Electric Circuits*, McGraw Hill, 4th Ed., 2009.
3. Paul, C., *Introduction to Electromagnetic Compatibility*, Wiley, 2006.

THE MANY ASPECTS OF SEMICONDUCTOR RELIABILITY WITH IMPACT ON ESD DESIGN

Charvaka Duvvury and Mirko Scholz on behalf of EOS/ESD Association, Inc.

Many articles published in *In Compliance* focus on ESD design and testing methods. But there is a lot more to semiconductor reliability. ESD reliability is based on the understanding of the high current behavior of protection devices. Protection designs are implemented in the IC to meet the ESD targets. This approach is not feasible for most of the other semiconductor reliability phenomena. In contrast to ESD, the actual understanding and definition of semiconductor reliability for field applications is less precise. It requires the understanding of device physics and reliability models. These models are mostly established and allow with some confidence to predict the IC device lifetime during field applications. In this article, we will have a look at different reliability phenomena and models and their contribution to the overall semiconductor reliability. We specifically cite only three representative references here [1-3] although the literature has an immense amount of work on the different reliability aspects, especially exhaustively covered by the technical papers at the International Reliability Physics Symposium for the last five decades.

The major reliability concerns for CMOS technologies include Hot Carrier Injection (HCI), Gate Oxide Reliability (GOX), Electro-migration (EM), Negative Bias Temperature Instability (NBTI), and Latchup (LUP). A more uniquely different topic is Electrical Overstress (EOS). EOS is often caused by misapplications as reported by the white paper from the Industry Council [4]. For example, the maximum voltage applied on the supply pin exceeds its absolute maximum voltage rating or AMR. This can cause latchup and high thermal stress and eventually lead to an EOS damage.

Figure 1 links all of these in a visual manner. ESD reliability is purposely placed at the centre although this is not necessarily true for every IC product development. In fact, often ESD is addressed after a

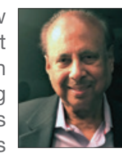

Charvaka Duvvury, IT2 Technologies, is a fellow of the IEEE and works as a technical consultant on ESD design methods and ESD qualification support. He received his Ph.D. in engineering science from the University of Toledo. He has published over 150 papers in technical journals and conferences and holds 75 patents. He is co-founder and co-chair of the Industry Council on ESD Target Levels.

Dr. Mirko Scholz, Infineon Technologies AG, received his Ph.D. in Electrical Engineering from the Vrije Universiteit in Brussels (VUB). He has authored/co-authored more than 100 publications, tutorials, and patents in the field of ESD design and testing. He is a regular reviewer for several IEEE journals and a current member of the IRPS sub-committee on ESD and Latchup.

Founded in 1982, EOS/ESD Association, Inc. is a not for profit, professional organization, dedicated to education and furthering the technology Electrostatic Discharge (ESD) control and prevention. EOS/ESD Association, Inc. sponsors educational programs, develops ESD control and measurement standards, holds international technical symposiums, workshops, tutorials, and foster the exchange of technical information among its members and others.

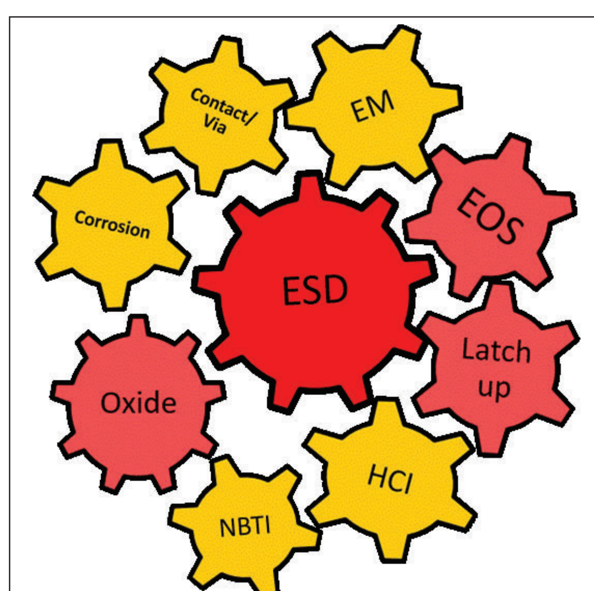

Figure 1: Interrelations between the various IC reliability effects

reliable process technology is established. As shown in the figure the reliability issues are all interconnected to both EOS and ESD although not necessarily in the same manner or to the same extent. Each of these reliability aspects have to be first considered separately before the connections to ESD and/or EOS can be understood.

HCI (noted as CHC in the figure) is related to degradation of transistor conductance during long-term operation caused by hot electron injection near a high field drain junction in a transistor. HCI can be mitigated with engineering of the drain junction with lightly doped drain (LDD) or graded junction implants that reduce the drain electric field. This improvement is a result of reduced peak substrate current ISUB. Incidentally, ISUB in turn plays a role on ESD and Latchup designs because of its impact on the parasitic bipolar transistor.

GOX reliability includes two issues: GOX breakdown and time-dependent-dielectric-breakdown (TDDB). GOX breakdown occurs when the applied voltage (or electrical field) exceeds the dielectric strength of the GOX. It can also suffer from a slow breakdown during its lifetime at normal operating voltages. This phenomenon is known as TDDB. Both of them are impacted by ESD stress either in magnitude, duration or in repetition. Therefore, ESD is a serious concern for GOX reliability and the oxide breakdown voltage is a main design input during ESD protection design.

NBTI is a serious concern for CMOS technologies starting at the sub-500nm nodes and for PMOS transistors that mostly operate in gate-to-source voltage mode. It can lead to a degradation of the trans-conductance. Consequently, if a large PMOS transistor is used as an ESD clamp in MOS conduction mode it should be characterized for NBTI effects.

The parasitic interaction between NMOS and PMOS can form a lateral *pnpn* device or thyristor. A turn-on of this thyristor during normal IC operation can lead to LUP. Ironically, this *pnpn* is also used as a well-known ESD protection device, the Silicon Controlled Rectifier (SCR). The substrate also plays a critical role for Silicon on Insulator (SOI) technologies developed to mitigate LUP in very advanced technology nodes. The use of the buried oxide in SOI technologies can have an adverse impact on ESD due to self-heating effects.

EM is a result of current conduction with a high current density through metal lines. It is strongly impacted by the interconnect technology. During ESD and EOS events a metal line temporarily heats up. This can lead to a degradation of its EM lifetime. To avoid these effects, a reliable ESD design requires sufficient wide metal lines. Both ESD and EOS can also cause contact burnout or via migration. Technology process changes with barrier metals such as Titanium or Tungsten are developed to prevent contact spikes and increase the reliability of these interconnects.

There are also reliability issues at IC package level. Materials, package type, electrical bias, operation temperature and environmental conditions during normal operation of the IC can affect the corrosion of metals and mechanical stress in the package during its lifetime.

In conclusion, there are various reliability issues in semiconductor devices. In contrast to ESD, most reliability issues are not solved by design but solely with the help of predictive reliability models. Reliability issues need to be continuously addressed during technology development as technologies further advance into novel transistor structures such as FinFETs and Multi-gate devices.

REFERENCES

1. C. Hu et al., “Hot-electron induced MOSFET degradation - Model, monitor, and improvement,” IEEE Tran. Elec. Dev., ED32, P. 375, 1985.
2. A. Ille, W. Stadler, A. Kerber, T. Pompi, T. Brodbeck, K. Esmark and A. Bravix, “Ultra-thin gate oxide reliability in the ESD time domain,” EOS/ESD Symposium, pp. 285-294, 2006.
3. K. Banerjee, A. Amerasekera, and C. Hu, “Characterization of VLSI circuit interconnect heating and failure under ESD conditions,” Reliability Physics Symposium, 1996, 34th Annual Proceedings, IEEE International, pp. 237-245.
4. JEDEC Document, JEP 174, “Understanding Electrical Overstress – EOS.”

Banana Skins

411 Brake failure due to illegally modified transceivers suspected of causing two bus accidents

It has been reported widely in the Japanese press that electromagnetic interference caused by illegally modified transceivers on trucks is suspected of causing two accidents by disabling the braking system of commuter buses.

Mitsubishi Fuso Truck & Bus Corporation announced that two models of its buses are adversely affected by high-powered EMI from short distance and its braking system may not function properly under such conditions. Specifically, its breaking system that detects the wheel-locking condition falsely triggers due to the EMI and thus the brake doesn't work as intended.

Two accidents were reported last year where the bus drivers reported that the brake suddenly stopped working. However, after the police investigation, no visible malfunction was found.

The manufacturer continued investigation and found that high-powered radio signals emitted by a nearby transceiver (illegally modified and thus 1,000-10,000 as strong as permitted by law for such transceivers) can interfere with its braking control unit, resulting in false information that the wheels locked due to braking. Upon this false information, it seems (my interpretation from what I read various reports) that the control unit decided to release the brakes, and thus caused unintended loss of braking.

It is not known whether such illegally modified transceivers were present nearby in two accident cases. But in other two instances where loss of braking was observed, the bus drivers saw suspicious trucks nearby.

The company could reproduce the condition in live experiments, and it will refit the 2200+ cars by replacing the control unit, sensors, pipes, circuit harness, etc. I think the company should be commended for its continued investigation after the accidents.

I have personally noticed voices of presumably truck drivers whose transceiver must have been modified to generate enormous amount of power from my audio equipment over the years. (Remember the CB radio craze of 1970's?) But this is the first time such strong emission is linked to real-world accidents. [I don't think so. We had CB interference knocking out cruise controls long ago. PGN]

The warning that I see and hear on airplanes during landing and take off is no longer a remote worry. I should be glad that most air runways seem to have enough distance from the nearby highway.

As we depend on computers and sensors for better control of *everything* such as cars, home appliances, the malfunctions due to external EMI must be considered carefully, but I suspect that only the military agencies who have tried to harden the fighter planes and such against the EMI caused by nuclear blasts have the technical knowhow or mentality to cope with such problems caused by unusually and possibly illegally high-powered EMI.

(Yes, I know that the FCC regulations and similar usually protect the ordinary home appliances against the run-of-the-mill EMI from computers, etc. However, I doubt that electronic home appliance makers are ready to tackle the above the normal, high-powered emission caused by illegally modified transceivers. And they are a real threat along busy traffic route today. I hate to see various home appliances behave erratically every time a truck with such a transceiver passes by. Or for that matter, a whole field filled with tiny sensors blown by a strong zap of an illegally modified transmitter. Illegal or not, such dangers are going to be real and may have wide-spread consequences in the future.)

(Copied entire from "Loss of bus braking due to nearby illegally modified transceivers", The Risks Digest, Volume 23: Issue 9, 23 December 2003, posted by Chiaki, ishikawa@yk.rim.or.jp, 21 December 2003, brought to our attention by Simon Brown of the Health and Safety Executive, HSE. Current issues of The Risks Digest, which is a 'moderated usegroup' can be read at https://catless.ncl.ac.uk/risks. Also see Banana Skin No. 331.)

412 Car key fob malfunctions weather or interference from Wi-Fi hub?

A friend parked her Mitsubishi FTO at our house after a 30-mile drive in pouring rain. When she tried to lock the car, her electronic fob would not work (she could secure the car manually, but was unable to restart without the remote). We called in an emergency service, but it could not solve the problem. Then our neighbour arrived home in his Nissan pick-up and his fob wouldn't work either. This had never happened before. At the same time his wire-free doorbell had been going crazy and had to be disconnected. This made us suspicious, so we carried out a few tests. The key fobs worked on my Ford Mondeo and my neighbour's Range Rover. My neighbour drove his pick-up about 100 yards down the road and the key fob started working again, but when he returned it didn't. We then rolled the Mitsubishi down the road and the key fob duly worked, but it ceased to function once again when she returned to our house. When she left six hours later, the weather had dried and the Mitsubishi fob worked perfectly. What might have caused this?

Banana Skins *continued*

'Honest John' replies: It was possibly the result of an electrical field conducted by the rainwater. But are you sure no one nearby was using a wireless internet hub?

(From 'Honest John', Telegraph Motoring, February 10 2007, page M9.)

413 Radio microphone interferes with bingo hall sound system

There is no escape from the climate change debate. Regulars at an Islington bingo hall ("two women of weight – 88") were enjoying a mild flutter when suddenly the fruity tones of The Guardian's George Monbiot came over the loudspeaker with his customary message of doom.

Monbiot was conducting an interview at Greenpeace HQ next door, using a radio mike. No need to interrupt the fun, though – eyes down for a fully-insulated, more climate-friendly house.

(Roland White, "Climate change bingo flutter" in the 'Atticus' column, The Sunday Times, February 11th 2007, page 19.)

414 'First Responder' frequency tests interfere with garage door openers

The Associated Press reports that recent testing by the U.S. Air Force of radio frequencies intended for eventual use by first responders has had the unintended effect of disabling automatic garage door openers in an area near Colorado Springs, CO.

The frequency testing in late November 2006 reportedly took place at the Cheyenne Mountain Air Station, the location of the North American Aerospace Defence Command. The effects from the transmission should technically have been limited an area 15 kilometers from the test site, but Air Force officials suspect that the affected range was extended due to the height of the testing site (nearly 2000 meters).

As a result, hundreds of residents in the area surrounding the Station found their automatic garage door openers suddenly inoperable. One area company reportedly received more than 400 phone calls for assistance in fixing the disabled garage door openers.

Air Force officials are said to be investigating how best to resolve the interference problem, and have discontinued the frequency testing for now.

(Copied entire from Conformity magazine, January 11, 2007. Wikipedia says: "A certified first responder is a person who has completed forty to sixty hours of training in providing care for medical emergencies. They have more skill than someone who is trained in first aid but are not emergency medical technicians." In the UK they are called the Emergency Services.)

The regular "Banana Skins" column was published in the EMC Journal, starting in January 1998. Alan E. Hutley, a prominent member of the electronics community, distinguished publisher of the EMC Journal, founder of the EMCIA EMC Industry Association and the EMCUK Exhibition & Conference, has graciously given his permission for In Compliance to republish this reader-favorite column. The Banana Skin columns were compiled by Keith Armstrong, of Cherry Clough Consultants Ltd, from items he found in various publications, and anecdotes and links sent in by the many fans of the column. All of the EMC Journal columns are available at https://www.emcstandards.co.uk/emi-stories, indexed both by application and type of EM disturbance, and new ones have recently begun being added. Keith has also given his permission for these stories to be shared through In Compliance as a service to the worldwide EMC community. We are proud to carry on the tradition of sharing Banana Skins for the purpose of promoting education for EMI/EMC engineers.

PRODUCT Showcase

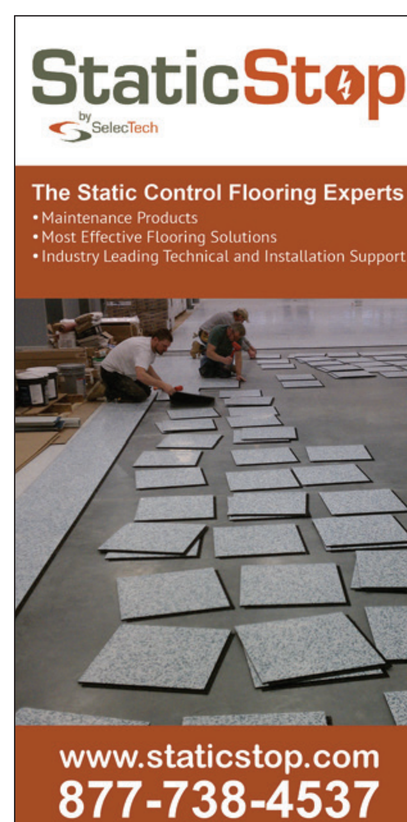

Advertiser Index

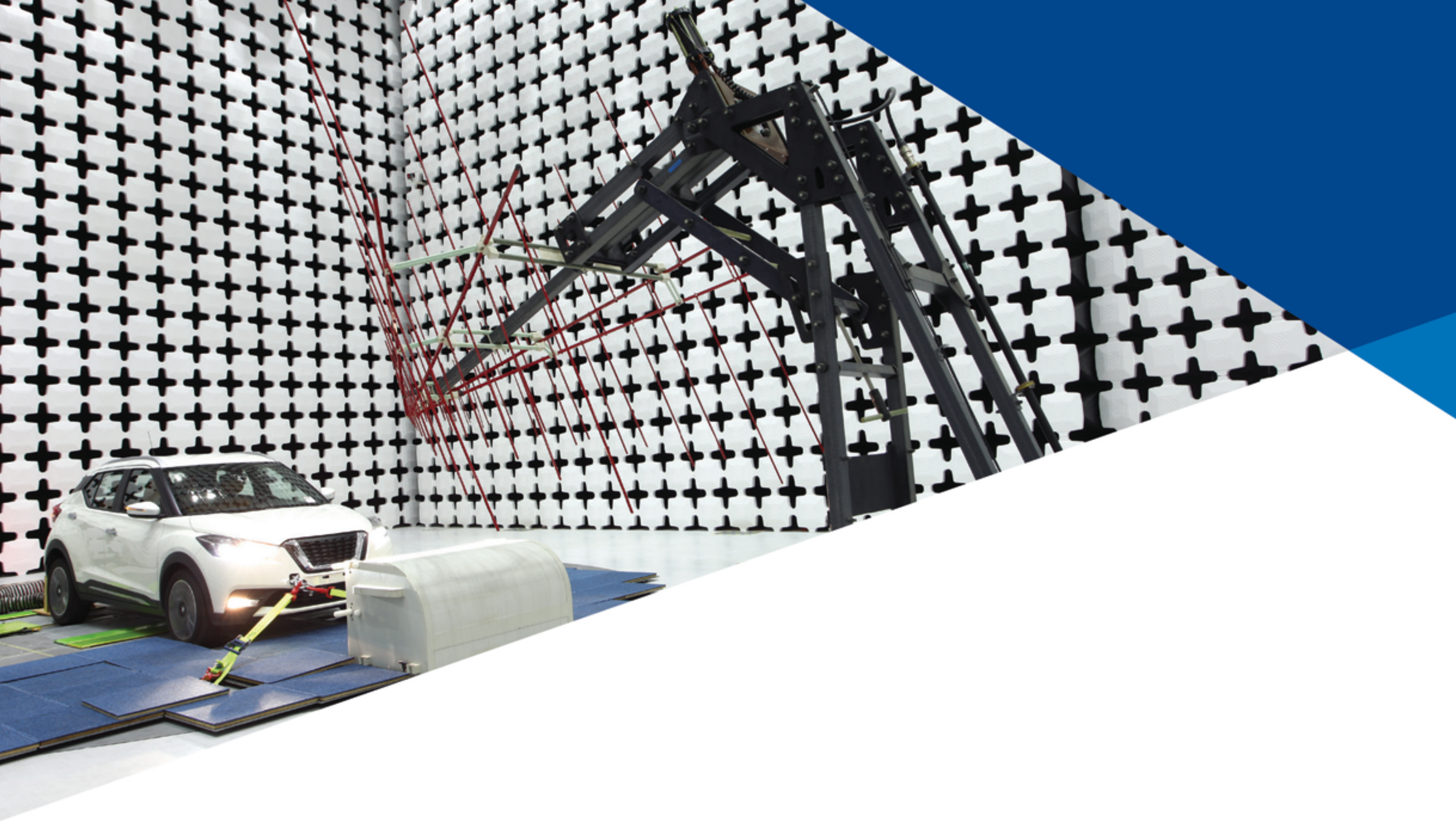

COMMITTED TO A SMARTER, MORE CONNECTED FUTURE

From electric vehicles to self-driving technology to drones performing routine deliveries, our lives are increasingly dominated by EMC. So, too, is ETS-Lindgren's commitment to measurements and compliance testing. Surpassing the standards of EMC performance, ETS-Lindgren is Committed to a Smarter, More Connected Future.

As an international manufacturer of market-leading solutions and products that measure, shield, and control electromagnetic and acoustic energy, ETS-Lindgren is the driving force allowing industry innovators to develop the latest technological advances and meet compliance standards. From chambers to test cells, absorbers, positioners, antennas, and software, ETS-Lindgren's EMC solutions are intelligently designed for reliability, diversity, ingenuity, and precision.

More importantly, our ability to create real-world test scenarios, troubleshoot potential failures, perform production testing, and maximize the chance of passing standards on time and on budget helps our customers bring life-changing products to market – faster.

For more information on our EMC solutions, visit our website at www.ets-lindgren.com/industries/emc-testing.

Connect with us at:

COMMITTED TO A SMARTER, MORE CONNECTED FUTURE

ETS·LINDGREN®
An ESCO Technologies Company

Offices Worldwide | **ets-lindgren.com**